

# Evaluation of long-term carbon dynamics in ~~afforested~~a drained peatlands: ~~Insights from~~forested peatland using the ForSAFE-Peat Model.

Daniel Escobar<sup>1,2</sup>, Stefano Manzoni<sup>1</sup>, Jeimar Tapasco<sup>2</sup>, Patrik Vestin<sup>3</sup>, Salim Belyazid<sup>1</sup>

<sup>1</sup> Department of Physical Geography and Bolin Centre for Climate Research, Stockholm University, SE-106 91 Stockholm, Sweden.

<sup>2</sup> Climate Action, Alliance of Bioversity International and the International ~~Center~~Centre for Tropical Agriculture (CIAT), Palmira 763537, Colombia.

<sup>3</sup> Department of Physical Geography and Ecosystem Science, Lund University, SE-22362 Lund, Sweden.

Correspondence to: Daniel Escobar (daniel.escobar@natgeo.su.se)

**Abstract.** ~~Afforested~~Management of drained ~~forested~~ peatlands ~~have significant~~has important implications for ~~greenhouse gas~~(GHG)carbon budgets, ~~with~~but contrasting views ~~exist on their~~its effects on climate. This study ~~utilized~~utilised the dynamic ecosystem model ForSAFE-Peat to simulate biogeochemical dynamics over two ~~full~~complete forest rotations (1951-2088) in a nutrient-rich drained peatland afforested with Norway spruce (*Picea abies*) in southwest Sweden. Model simulations aligned well with observed groundwater levels ( $R^2 = 0.7478$ ) and soil temperatures ( $R^2 \geq 0.7876$ ), and captured seasonal and annual net ecosystem production patterns, although daily variability was not always well represented. ~~Model outputs were analysed under~~Simulated carbon exchanges (a positive sign indicates gains and a negative sign indicates losses) were analysed considering different system boundaries (soil, ecosystem, and ecosystem plus the fate of harvested wood products, named ecosystem+HWP) ~~to assess carbon exchanges~~ using the net carbon balance (NCB) and the integrated carbon storage (ICS) metrics. ~~Results~~Model results indicated negative NCB and ICS across all system boundaries, except for a positive NCB calculated by the end of the simulation at the ecosystem+HWP level. The soil exhibited persistent carbon losses primarily driven by peat decomposition. At the ecosystem level, net carbon losses were reduced as forest growth partially offset soil losses until harvesting. NCB was positive (~~40152307~~  $\text{gC m}^{-2} \text{soil}$ ) at the ecosystem+HWP level due to the slow decay of harvested wood products, but ~~a~~ICS was negative ~~ICS~~ (~~-7(-0~~ $\times 10^5.59 \times 10^6$   $\text{gC yr m}^{-2} \text{soil}$ ) due to ~~the large~~ initial carbon losses. This study highlights the importance of system boundary selection and temporal dynamics in assessing the carbon balance of ~~afforested~~forested drained peatlands.

## 1 Introduction

Atmospheric greenhouse gas (GHG) concentrations consistent with the Paris Agreement's long-term temperature goal require ambitious carbon removals during this century (Rogelj et al., 2018). Land management practices can lead to net removals or

net exports depending on several controlling factors, often hard to quantify and ~~generalize~~generalise (Crusius, 2020; Guenther et al., 2020; Krause et al., 2020; Seddon et al., 2020). This problem is particularly acute in peatlands, as they are ~~both~~-large carbon stores and ~~are~~ very sensitive to land management.

Forestry on drained peatlands is a widespread land management practice in the northern hemisphere, covering approximately 15 million hectares, and it has significant~~important~~ implications ~~on GHG~~for carbon budgets (Leifeld et al., 2019). This practice is ~~especially common~~widespread in ~~northern Europe, covering Fennoscandia, spanning~~ around 5.7, ~~1.5 and 0.3~~ million hectares in Finland; and 1.5 million hectares in Sweden and Estonia respectively (Vasander et al., 2003). Drainage leads to important changes in the carbon dynamics of these systems (Ojanen & Minkinen, 2019). Lowering the water table promotes forest growth and, subsequently, carbon accumulation in living biomass ~~in addition to decreasing and decreases~~ methane emissions; (Escobar et al., 2022). Nonetheless, higher soil oxygen content associated with lowering the water table promotes decomposition, potentially leading to substantial carbon emissions from peat soils (~~He et al., 2016~~)(He et al., 2016). According to Jauhiainen et al. (2023), the soil carbon balance, calculated as the difference between litter inputs and heterotrophic respiration, commonly shows soil carbon losses for ~~afforested peat soils on drained forested peatlands at~~ northern latitudes, ranging from 21 and 261 gC m<sup>-2</sup> yr<sup>-1</sup> depending ~~on~~of climate and nutrient status.

Restoration of water table levels and wetland vegetation has been proposed ~~as a tool for meeting to meet~~ Paris Agreement targets (Guenther et al., 2020; Tanneberger et al., 2021). Several efforts to restore peatlands are underway. For example, the EU Nature Restoration Law has proposed specific area targets for peatland rewetting (Noebel, 2023). Drained peatlands restored through rewetting exhibit long-lasting differences regarding hydrological and ecological dynamics compared to their pre-drainage status (Kreyling et al., 2021). However, restoration seems capable of reducing soil carbon losses in these systems (Darusman et al., 2023; Escobar et al., 2022).

While restoration through rewetting holds promise for mitigating climate change, its effectiveness remains a subject of debate due to different views about the effects on climate caused by ~~afforested~~-drained forested peatlands ~~in at~~ northern latitudes (Kasimir et al., 2018; Meyer et al., 2013; Ojanen & Minkinen, 2020). Whether all types of drained peatlands consistently lose soil carbon is still an open question due to contrasting results from field measurements (Butlers et al., 2024; Hermans et al., 2022; Meyer et al., 2013; Minkinen et al., 2018). Additionally, disagreement persists regarding the appropriate boundaries for analysing these ~~systems~~systems, specifically whether carbon accumulated in harvested tree biomass should be included in the carbon budgets ~~of these systems~~ to estimate ~~their impact on~~-climate ~~during~~impacts in a timeframe relevant ~~for to~~ climate change mitigation (Kasimir et al., 2018; Ojanen & Minkinen, 2020).

The importance of the tree biomass components is clear from net ecosystem production (NEP) measurements performed with the eddy covariance technique, which indicate a persistent carbon sink in ~~afforested~~-drained forested peatlands despite high soil carbon losses (Korkiakoski et al., 2019; Meyer et al., 2013; Tong et al., 2024). It has been ~~recognized~~recognised that in cases of persistent and large soil carbon losses, compensation through forest carbon uptake is limited because the tree component has a maximum carbon storage capacity lower than the carbon stocks of ~~a~~-typical peat soil. The magnitude and extent of this compensation are likely sensitive to how harvested wood products (HWP) are accounted for. When considering

Field Code Changed

Formatted: Swedish (Sweden)

Formatted: Swedish (Sweden)

65 HWP, post-harvesting periods are of special ~~relevant~~relevance, suggesting that ~~to understand the trade-off between tree biomass carbon and soil carbon,~~ it is necessary to analyse carbon dynamics over more than one forest rotation: ~~to understand the trade-off between tree biomass carbon and soil carbon.~~ This shows how differences in system boundary definition, meaning considering the carbon balance within the soil, ecosystem, or the ecosystem plus the fate of HWP, may lead to contrasting results.

70 Furthermore, due to tree carbon uptake compensation of soil carbon losses, the effects on the climate of these systems might be greatly affected by how the forest stand is managed (Tong et al., 2024), which adds uncertainties to the estimated carbon budgets. ~~Indeed, a large area of drained afforested peatlands is likely to undergo conventional forest management in the next few decades. Indeed, a large area of drained forested peatlands will likely undergo conventional forest management in the next few decades (Lehtonen et al., 2023).~~ Field-based measurements of carbon balances have shown high temporal variability due

75 to high sensitivity to nutrient status, forest stand characteristics, water table level and temperature (Korkiakoski et al., 2023; Mamkin et al., 2023). Adding to these uncertainties, measurements are usually performed during short periods (Escobar et al., 2022) that do not correspond to the long cycles of conventional forestry. ~~Utilizing~~To complement short-term measurements, dynamic ecosystem models can provide simulation data about carbon dynamics representative of long periods that can be further ~~being~~ analysed under different system boundaries ~~to complement short-term measurements~~ (Minkinen et al., 2018).

80 Here, we introduce the dynamic ecosystem model ForSAFE-Peat and use it to analyse long-term carbon dynamics in a drained forested ~~drained~~ peatland. ~~Several~~ForSAFE-Peat builds on previous models ~~have been developed to represent of~~ carbon dynamics ~~of in~~ coniferous forest and peat soils. ~~ForSAFE-Peat integrates many common assumptions often use in these models and is our objective to reflect on their effects on the simulated carbon dynamics. ForSAFE-Peat. It~~ simulates plant dynamics as a big leaf model where photosynthesis is a function of foliar nitrogen content ~~using the same structure of as in~~ the PnET

85 model (Aber & Federer, 1992). This representation has been widely use to study managed coniferous forest in northern latitudes (Belyazid et al., 2011; Belyazid & Zanchi, 2019; de Bruijn et al., 2014; Gustafson et al., 2020). ForSAFE-Peat simulates ~~soil~~the soil as a groupset of layers that can expand or contract due to soil organic matter content changes ~~similarly than in, similar to~~ peat development models like HPM (Frolking et al., 2010). Soil organic matter is represented by several compartments, ~~where the including litter that, during~~ decomposition ~~flux of compartments that represent litter fill a pool that~~ represents, provides carbon and nutrient inputs to peat pools, resembling approaches like the one implemented in Yasso07

90 (Didion et al., 2014). This allows a simple representation of litter quality and peat. Decomposition is described ~~with linear kinetics as a first-order exponential decay process~~ where the peat decomposition rate constant is the same ~~that has been~~ used to evaluate future carbon dynamics of northern peatlands by land-surface models such as ORCHIDEE (Qiu et al., 2018) and LPJ-GUESS (Chaudhary et al., 2022). ~~By building on existing state-of-the-art models, ForSAFE-Peat follows traditional~~ assumptions, making it a suitable tool for exploring carbon dynamics in peatland systems and critically examining commonly

95 used methods for their representation.

In this study, we used the ForSAFE-Peat model to conduct a long-term simulation spanning two complete forest rotations in a well-studied drained forested peatland in southwest Sweden, utilising primarily pre-calibrated parameters. Model outputs were

analysed to represent various system boundaries and different metrics were applied to evaluate carbon exchanges across these boundaries. While acknowledging the potential significance of N<sub>2</sub>O emissions in drained fertile peatlands (Jauhiainen et al., 2023), we In this study, we used the ForSAFE-Peat model to conduct a long-term simulation spanning two full forest rotations in a well-studied drained and afforested peatland in southwest Sweden, utilizing primarily pre-calibrated parameters. Model outputs were analysed to represent various system boundaries, and different metrics were applied to evaluate carbon exchanges across these boundaries. Consequently, we explore the following two questions in this contribution

In this contribution, we address the following questions:

Do model outputs resemble focused on carbon dynamics. Consequently, we explore the following two questions:

- i. How well does ForSAFE-Peat reproduce field-based observations of soil and vegetation related to carbon dynamics in a northern drained afforested/forested peatland?
- ii. Do model outputs indicate different How do patterns of modelled carbon exchange vary across different system boundaries for in a northern afforested drained forested peatland?

## 2 Methods

We modified the forest ecosystem model ForSAFE (Wallman et al., 2005; Zanchi, et al., 2021b) to better describe prominent processes in peat soils. We then used the modified model ForSAFE-Peat to simulate biogeochemical dynamics encompassing two full/complete forest rotations of in a drained nutrient-rich peatland dominated by planted with Norway spruce (*Picea abies*).

Site conditions were typical of afforested-drained forested peatlands in southwest Sweden under conventional forestry management practices.

For the first question, we compared model outputs to field measurements performed in a heavily an intensively monitored site using goodness of fit indicators. For the second question, we used model outputs to quantify two carbon exchange metrics under different system/system boundaries and we analysed their evolution throughout the period of analysis time.

### 2.1 Model description

ForSAFE-peat simulates daily biogeochemical dynamics building upon the established ForSAFE model (Wallman et al., 2005; Yu et al., 2018; Zanchi, et al., 2021b). This process-based and compartmental model tracks carbon, water and nutrient flows throughout a forest stand ecosystem. A detailed description of the model and its mathematical formulation can be found in the supplementary information section Supplementary Information 1; here, we only provide a short summary.

The model simulates daily photosynthesis as a function of photosynthetically active radiation-regulated by, temperature, leaf area, foliar nitrogen content, water availability, and atmospheric CO<sub>2</sub> concentration. Photosynthesized/Photosynthesised carbon and assimilated nutrients are initially allocated within five labile compartments before entering four specific plant compartments (leaves, branches, wood, and roots). Carbon and nutrients are either harvested or return-to-the/returned to the soil

through litterfall for further cycling through decomposition. Woody residues associated ~~to management removals with thinning~~  
130 ~~and harvest~~ are allocated to an intermediate compartment of deadwood before entering the soil as litter.

Soil is represented by layers defined by the user, and each ~~layer's layer~~ thickness is allowed to vary during the simulation based  
on the amount of organic matter it holds while porosity remains constant. Heat is transported vertically according to the heat  
equation adapted for peat soils. Downward water movement is driven by gravity and modulated by soil hydrological properties,  
while plants influence water uptake through transpiration. Additionally, specific layers can exchange water horizontally,  
135 simulating the impact of ~~drainage ditches on hydrological processes within the peatland. ditching on hydrological processes~~  
~~within the peatland. The ditch function is simulated by setting an initial drainage depth. Layers above this depth experience~~  
~~lateral outflow when water content exceeds field capacity, with outflow regulated by the layer's hydraulic conductivity and~~  
~~width, as described in Zanchi et al. (2021b). The drainage depth adjusts dynamically with changes in the soil profile; when the~~  
~~soil profile height is reduced due to net losses of soil organic matter, the ditch depth is also reduced by the same magnitude.~~

Organic matter within the soil is divided ~~between among~~ four solid compartments (easily decomposable compounds, cellulose,  
140 lignin and peat) that are decomposed at different rates according to first-order kinetics modified by temperature, moisture, and  
pH. This process releases dissolved organic compounds (dissolved organic carbon, dissolved organic nitrogen and CH<sub>4</sub>) and  
mineral compounds (CO<sub>2</sub>, NH<sub>4</sub><sup>+</sup>, Mg<sup>+</sup>, K<sup>+</sup> and Ca<sup>+</sup>) into the soil solution. Mineral weathering ~~and~~ atmospheric deposition ~~and~~  
~~ion exchange further add, and in the latter may also remove, contribute~~ compounds such as sulphate (SO<sub>4</sub><sup>-</sup>), nitrogen ions (NH<sub>4</sub><sup>+</sup>,  
145 NO<sub>3</sub><sup>-</sup>), base cations (Mg<sup>+</sup>, K<sup>+</sup>, Ca<sup>+</sup>), chloride (Cl<sup>-</sup>), sodium (Na<sup>+</sup>) and aluminium (Al<sup>+</sup>) to the soil solution. ~~Soil solution pH~~  
~~is then calculated based on the acid neutralizing capacity of the soil solution. Atmospheric deposition, influenced by historical~~  
~~and local conditions, is a direct input of these compounds and ions. At the same time, mineral weathering depends on the~~  
~~mineral content, reducing its significance in organic soils with lower mineral availability. Additionally, ion exchange processes~~  
~~regulate the availability of these compounds through adsorption or desorption. Leaching, driven by water exports, removes~~  
150 ~~compounds from the soil solution.~~

Mass balance equations that account for gas-water partitioning, diffusion, water transport, plant uptake and chemical  
transformations are used to track the concentration of these elements in the soil. ~~Soil solution pH is then calculated based on~~  
~~the acid-neutralizing capacity of the soil solution.~~

The model tracks the fate of ~~the~~ carbon within the harvested biomass extracted from the site by allocating it into three  
155 compartments (fuel, fibre and ~~hard wood~~~~hardwood~~ products) whose decay is simulated through first-order kinetics and has  
~~not integrated no~~ feedback ~~to on~~ other parts of the model.

## 2.2 Site and scenario description

~~We simulated two forest rotations over the period from the beginning of 1951 to the end of 2088 at a drained afforested~~  
~~peatland located at Skogaryd Research Station (<https://meta.fieldsites.se/resources/stations/Skogaryd>) in the southwest of~~  
160 ~~Sweden (58°23'N, 12°09'E). This site has hemiboreal climate, high nutrient content organic soil, high peat depth, good~~

drainage, and conventional forestry management is adopted. The site, formerly a fen valley, underwent drainage in the late 19th century to facilitate agricultural use before being repurposed for forestry in 1951.

We simulated two forest rotations over the period from the beginning of 1951 to the end of 2088 at a drained afforested peatland located at Skogaryd Research Station (Klemedtsson et al., 2015) in the southwest of Sweden (58°23'N, 12°09'E).

This site experiences a hemiboreal climate, has nitrogen-rich peat soil, features an effective drainage system, and is managed under conventional forestry practices. Originally an open fen valley, the site was drained in the late 19th century for agriculture before being converted to forestry in 1951. The ditch network forms a grid-like pattern, with the main ditch running north to south for 0.8 km, draining into Lake Skottenesjön. Smaller parallel ditches are spaced at varying distances. Until clear-cutting in 2019, the site was dominated by Norway spruce (*Picea abies*). The area affected by clear-cutting covered approximately 0.16 km<sup>2</sup>, with logging debris left on most of the site (Figure 1). Norway spruce was replanted on 2/3 of the site following clear-cutting. In 2022, a barrier was constructed in the main ditch to raise the water level in the northern third of the site. Visual inspections revealed that vegetation cover increased in the years following clear-cutting. By 2022, much of the site remained covered by logging residues, while grasses and sedges, particularly in areas without logging debris, reached heights of 90 cm in the middle of the summer.

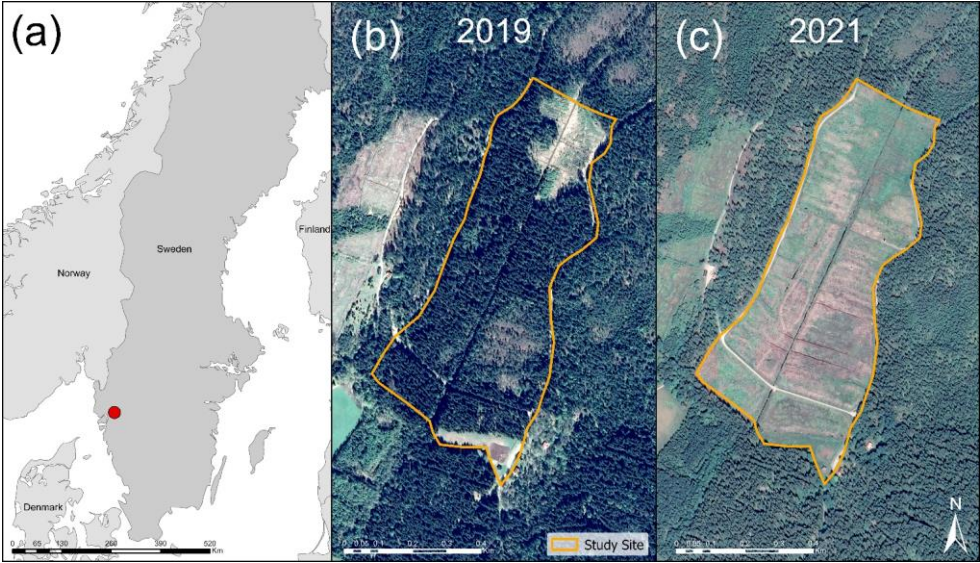


**Figure 1.** (a) Location of the Skogarvd Research Station in southern Sweden, marked with a red circle. (b) Satellite image of the study site in 2019, showing a predominantly coniferous forest. (c) Satellite image from 2021 after clear-cutting, revealing an extensive drainage network. Satellite images were obtained from Google Earth Pro.

The model used daily mean meteorological data (1951 to 2023) from the Swedish Meteorological and Hydrological Institute (SMHI) Vänernsborg (58°35'N, 12°35'E) and Uddevalla D (58°36'N, 11°93'E) and Vänernsborg (58°35'N, 12°35'E) stations, while future both located approximately 12 km from the site. Future climate data (2023 to 2088) were obtained from projections for forest sites under the CLEO research program (Munthe et al., 2016). Climate projections were downscaled from regional projections based on ECHAM and HADLEY climate model models under RCP 6.0 as in (Zanchi, et al., (2021a). RCP 6.0 represents a medium stabilisation pathway, where greenhouse gas emissions peak around 2080 and decline thereafter, reflecting a future with moderate climate change mitigation efforts. Yearly atmospheric deposition was derived from the MATCH model simulation (Engardt & Langner, 2013; Munthe et al., 2016) and scaled based on daily precipitation. Climate data used as an input for the simulations can be seen in Figure 2.

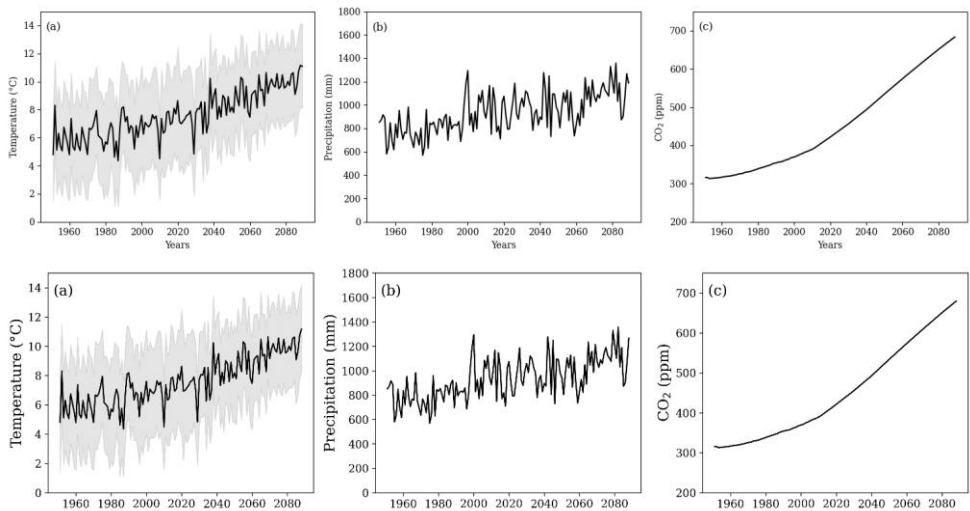


**Figure 2.** (a) Mean annual temperature (black line) and difference between mean annual maximum temperature and mean annual minimum temperature (grey area). (b) Annual precipitation. (c) Yearly average atmospheric CO<sub>2</sub> concentrations. The time series spans both the historical period (from 1951; data from the Swedish Meteorological and Hydrological Institute) and a future period (till 2088; data from model projections; see Section 2.2).

The simulated forest stand is assumed to consist entirely of Norway spruce. The modelled forest management mimicked replicated historical events at the site: spruce planting in 1951, a 72% tree biomass thinning in 1979, a 10% biomass



loss in 2010 due to storm damage, and a 96% biomass removal in 2019 due to a clear-cutting operation. Harvesting exerts important control over carbon dynamics in these systems. The large thinning event, which removed 72% of the biomass after approximately 28 years of plantation after planting, represents a non-conventional management practice (Metzler et al., 2024). This intensive management strategy was included in our simulations to accurately reflect the historical management of the real site on which our study is based. The second modelled rotation (2020–2088) followed the biomass removal time patterns of the first rotation. Simulation assumed Norway spruce (*Picea abies*) to be the only vegetation present at the site. Photosynthesis and plant growth parametrizations followed previous studies (Aber et al., 1996, 1997; Zanehi et al., 2021b). This intensive management strategy was incorporated into the simulations to accurately reflect the actual site's historical management. The second modelled rotation (2020–2088) followed the same biomass removal timing patterns as the first rotation.

The modelled soil profile, reflecting an average peat depth of 3 meters as reported by Nyström, (2016), for the site, was discretized into 10 layers. Of these, the top nine layers were initially 0.2 m thick, while the bottom layer had a thickness of 1.2 m. At the onset of the simulation, all layers were characterized by the same properties. Bulk density was uniformly set to  $0.20 \text{ g}_{\text{soil}} \text{ cm}^{-3}$ , informed by on-site observations and corroborated by findings in managed peat (Liu et al., 2020), while organic matter content was assumed to be 87%. Initial soil organic matter (SOM) was allocated entirely to the peat SOM compartment and 50% of it was assumed to be soil organic carbon (SOC). Initial soil organic matter (SOM) content was set to 87% based on Meyer et al. (2013) and mineral soil content was set to 13%. Initial SOM was allocated entirely to the peat SOM compartment, and 50% of it was assumed to be soil organic carbon (SOC), which implied an initial soil carbon density of  $0.08 \text{ g}_C \text{ cm}^{-3}$ . The initial carbon-to-nitrogen (C:N) ratio was set to 21, aligning with the observed average C:N at the site (Eriksson, 2021).

To simulate drainage, at the beginning of the simulation, the layers within a depth of 0.6 m had a lateral outflow of water controlled by their hydraulic conductivities. Because layers can expand or contract within the model structure due to changes in soil organic matter content, the fraction of the vertical soil profile subject to lateral flow changes through time. Ditch network maintenance (DNM) also results in changes in the layers from which lateral outflow is allowed. In order to mimic conventional management after clear-cut, we determined the soil layers within 0.6 m depth in 2022 and allowed horizontal water flow from them.

A more detailed description of the scenario parametrization can be found in the supplementary information section 2.

### 2.3 Simulation representativeness

We set the initial ditch depth at 0.6 m based on ditch depth estimations from previous work conducted at the site (He et al., 2016; Nyström, 2016). We aimed to simulate standard ditch network maintenance (DNM) practices. In reality, the ditch was not maintained after clear-cutting in 2019 due to a rewetting experiment that began in 2022. Therefore, NEP observations for 2020 and 2021 were made after clear-cutting and during a period without DNM. To integrate historical accuracy with our aim of representing conventional management practices, we reset the ditch depth to 0.6 m in our simulation starting in 2022. In the



model formulation, lateral drainage is influenced by changes in ditch depth, which reflect variations in soil profile depth and hydraulic conductivity due to changes in the bulk density of the layers susceptible to lateral drainage. In reality, ditch depth is also influenced by infilling caused by sedimentation, vegetation growth, and bank erosion (Hökkä et al., 2020). However, these processes are not incorporated into the model for the sake of simplicity. A more detailed description of the scenario parameterisation can be found in Supplementary Information 2.

### 2.3 Representativeness of model simulations

To evaluate the model's performance in replicating observed variables, we compared model outputs to available observations of abiotic factors controlling carbon dynamics and observations of carbon fluxes. For abiotic factors controlling carbon dynamics, we focused on soil temperature and ~~ground-water~~groundwater level (GWL), which are regarded as the main regulators of carbon fluxes in drained peatlands (Escobar et al., 2022; Evans et al., 2021; Jauhiainen et al., 2023). ~~Data for net ecosystem exchange representative NEP data~~ was available for the entire stand, ~~while. In contrast,~~ data for soil temperature and GWL ~~were available at from~~ several ~~distinct~~ locations at the site ~~which~~ were averaged for the numerical comparison with the model estimates. We ~~assessed~~calculated the coefficient of determination ( $R^2$ ) and the root mean squared error (RMSE), ~~as goodness of fit measures.~~

For on-site observations, daily ~~groundwater level~~GWL data spanning six years (2014-2020) were available at four distinct locations. Concurrently, ~~at three locations,~~ daily soil temperature records covering ~~a 14-year period years~~ (2008-2022) were obtained for three depths (0.05, 0.15, and 0.30 ~~meters~~ ~~at three locations m~~). Measurement methods used at the site are described in Ernfors et al. (2011) and Klemetsson et al. (2010). NEP (i.e. gross primary productivity minus ecosystem respiration) data were obtained from measurements done by eddy covariance ~~(EC) technique for the years.~~ On-site NEP measurements were conducted in 2008 while trees were present ~~on the site,~~ with subsequent data from 2020 and 2021 acquired post-clear-cutting, offering insights into soil respiration ~~in the absence of significant~~without substantial photosynthetic activity. ~~Data~~NEP data processing and acquisition ~~for the year 2008~~ is described in Meyer et al. (2013) and Vestin et al. (2020)Meyer et al. (2013). For the years 2020-2021, the high-frequency data needed for flux calculations were acquired with an ultrasonic anemometer (USA-1, METEK GmbH, Germany) and a LI-7200RS gas analyser (LI-COR Biosciences, NE, USA) mounted at 2.15 m height above the low vegetation. The data acquisition frequency was 10 Hz, and the half-hourly average  $\text{CO}_2$  flux was calculated with the EddyPro software, version 7.0.7 (LI-COR Biosciences, NE, USA) following the ICOS methodology (Sabbatini et al., 2018). Gaps in the dataset were subsequently filled using the REddyProCWeb online tool (Wutzler et al., 2018).

We performed manual calibration of two parameters: the modifier of the bottom layer hydraulic conductivity that controls percolation ( $\text{lim}K_{\text{sat}}$ ) and fraction of wood that respire ( $RWF$ ). Calibration was made against ground water level observations from two locations from 2008 to 2013 and informed by estimates of biomass on the site from 2008 to 2010 based on tree ring data (He et al., 2016). More information is provided in the supplementary information section 2

Formatted: English (United States)

ForSAFE-Peat calibration was intentionally limited, as the objective was to evaluate the outcomes of common modelling assumptions under the site's specific conditions that inspired our simulation. We manually calibrated two parameters: the modifier of the bottom layer hydraulic conductivity that controls percolation ( $limK_{sat}$ ) and the fraction of wood that respire ( $RWF$ ).  $limK_{sat}$  directly controls water leaving the soil profile by modulating percolation, thereby affecting the soil water balance.  $RWF$  influences autotrophic respiration, which affects the tree's carbon balance and, consequently, biomass. In turn, biomass impacts water uptake, influencing groundwater levels. The water table also affects biomass by controlling water availability and nitrogen mineralisation. Calibration of these two parameters was conducted by comparing model outputs to GWL observations from two locations (2008–2013) and to biomass estimates for the site (2008–2010) derived from tree ring data (He et al., 2016). Additional details are provided in Supplementary Information 2.

#### 2.4 Carbon exchange metrics and system boundaries

Two metrics related to the carbon balance were selected to evaluate the potential effects of carbon exchanges on climate: the net carbon balance (NCB) and the integrated carbon storage (ICS). The NCB is calculated as:

$$NCB(T) = \int_{t_0}^T [Ic(t) - Oc(t)] dt. \quad (1)$$

where  $NCB(T)$  is expressed in units of mass of carbon per ground area of reference ( $g_C m^{-2}_{soil}$ ) and is calculated as the carbon gain or loss after integrating the input fluxes of carbon ( $Ic(t)$ ) minus the outputs fluxes of carbon ( $Oc(t)$ ) from the beginning of the period of analysis ( $t_0$ ) until the end ( $T$ ).

The calculation of the  $ICS(T)$  shown in equation (2) can be interpreted as the cumulative carbon storage and is calculated by integrating the  $NCB(t)$  throughout the period of the analysis (Sierra, Muñoz et al., 2024),

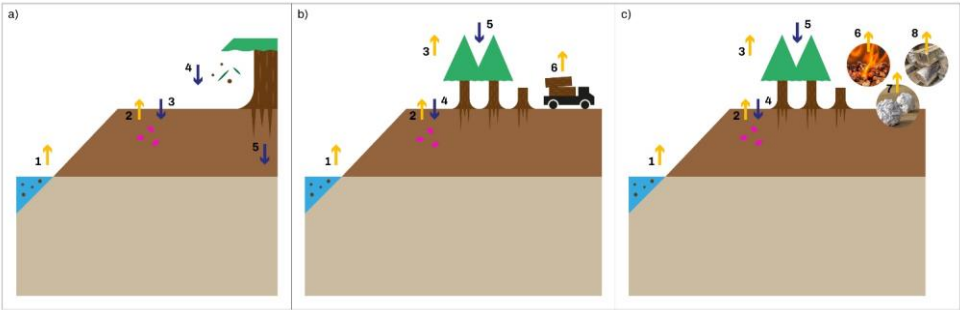
$$ICS(T) = \int_{t_0}^T NCB(t) dt \quad ICS(T) = \int_{t_0}^T NCB(t) dt. \quad (2)$$

Based on equation (2), this metric is expressed as mass of carbon per area multiplied by time ( $g_C \cdot yr \cdot m^{-2}_{soil}$ ). The  $ICS(T)$  is useful because it accounts for time dynamics of carbon storage, which in turn control the cumulative atmospheric cooling or warming effect a system has (Sierra, 2024; Sierra et al., 2021). When a system exhibits a very dynamic carbon exchange characterized by periods of large net losses and periods of large net gains, the  $NCB(t)$  might vary between positive and negative. The interval of time during which accumulated losses exceed accumulated gains can be interpreted as a period of negative effects on climate while the opposite is true for the interval of time during which accumulated gains exceed accumulated losses. This is captured by the  $ICS(T)$  by integrating the  $NCB(t)$  through a reference time period ( $T$ ).

Field Code Changed

Based on equation (2), this metric is expressed as the mass of carbon per ground area multiplied by time ( $\text{g}_\text{C} \text{ yr m}^{-2}_{\text{soil}}$ ). The  $ICS(T)$  is useful because it accounts for the time dynamics of carbon storage, which in turn control the cumulative contribution of a system to atmospheric cooling or warming (Muñoz et al., 2024; Sierra et al., 2021). When a system exhibits a very dynamic carbon exchange characterised by periods of large net losses and periods of large net gains, the  $NCB(t)$  might vary between positive and negative. The interval of time during which accumulated losses exceed accumulated gains can be interpreted as a period of negative effects on climate, while the opposite is true for the interval of time during which accumulated gains exceed accumulated losses. The cumulative effect of fluctuations in carbon storage is captured by the  $ICS(T)$  via integration of  $NCB(t)$  throughout the time period from  $t_0$  to  $T$ . ICS has been proposed to account for carbon permanence in a system (Fearnside et al., 2000). Studies like Sierra et al. (2021) have shown that ICS can effectively account for the time carbon spends stored in ecosystems, providing a more comprehensive means of analysing and comparing trajectories of carbon accumulation (Muñoz et al., 2024).

We estimated the previously explained metrics for three different system boundaries: the soil, the ecosystem and the ecosystem plus the fate of HWP, including harvested wood products (ecosystem+HWP). Differences in system boundaries imply different inflows and outflows ~~for~~of carbon as quantified by equation (1). By examining different system boundaries, we can offer diverse perspectives on the carbon exchanges (and thus the potential effect on climate) of ~~afforested~~-drained ~~forested~~ peatlands. Additionally, these delineations provide valuable categories for analysing the temporal dynamics of carbon fluxes and their associated controlling factors. Differences in system boundaries are represented and explained in Figure 3.



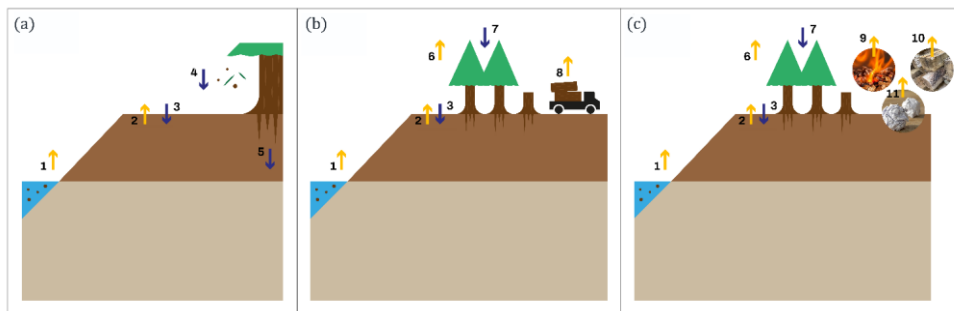


Figure 3. System boundaries used in the study: (a) Soil boundary, (b) Ecosystem boundary, and (c) Ecosystem + ecosystem + harvested wood products (HWP) boundary. Yellow arrows represent carbon outflows, and blue arrows represent carbon inflows. Soil boundary (a): carbon leaching (arrow 1), soil-atmosphere carbon exchange (arrows 2 and 3), litterfall (arrow 4), and belowground autotrophic respiration (arrow 5). Ecosystem boundary (b): carbon leaching (arrow 1), above-ground autotrophic respiration (arrow 3), soil-atmosphere carbon exchange (arrows 2 and 4), photosynthesis (arrow 5), tree harvesting (arrow 6). Ecosystem + HWP boundary (c): carbon leaching (arrow 1), above-ground autotrophic respiration (arrow 3), soil-atmosphere carbon exchange (arrows 2 and 4), photosynthesis (arrows 5 and 7), harvested biomass (arrow 8), and outflows from the decay of HWPs (arrows 9, 10 and 11).

Formatted: Strong

Formatted: Font: Not Bold

Leached carbon might be in the form of dissolved methane ( $\text{CH}_4$ ), carbon dioxide ( $\text{CO}_2$ ) and dissolved organic carbon (DOC). Furthermore, we considered the gas exchange of  $\text{CO}_2$  and  $\text{CH}_4$  between the atmosphere at the soil which can be outflow or inflow based on the concentration gradient. We did not account for chemical transformations of leached carbon that can happen in ditches and streams. For all these system boundaries, outputs are indicated by negative fluxes and inputs by positive fluxes. For all system boundaries, outputs are represented by negative fluxes and inputs by positive fluxes. The soil boundary includes inflows from litterfall and belowground autotrophic respiration, with outflows from leached carbon (e.g., dissolved organic carbon,  $\text{CO}_2$ , and  $\text{CH}_4$ ). Soil-atmosphere carbon exchange is gradient-controlled and can act as either an input or output of gaseous carbon ( $\text{CO}_2$  and  $\text{CH}_4$ ). At the ecosystem boundary, photosynthesis is an inflow, while leaching, aboveground autotrophic respiration and harvested biomass are outflows. Soil-atmosphere exchange is also included. The ecosystem+HWP boundary accounts for the same fluxes as the ecosystem boundary, but harvested biomass is replaced by the decay of wood products.

### 3 Results

#### 3.1 Simulation representativeness

##### 3.1 Representativeness of model simulations

The model captured daily observations of groundwater table and soil temperature relatively well, but less so for daily NEP. However, simulated annual and seasonal NEP are closely comparable to the observations.

### 3.1.1 Abiotic factors

Observed groundwater levels (GWL) from 2014 to 2021 had a mean of  $-0.4540$  m and a standard deviation of  $0.17$  m. Only considering the period before clear-cutting (2014–2019), observed GWL had a mean of  $-0.45$ . Summer lower values before clear-cutting ranged between  $-0.6$  and  $-0.9$  m. The high summer groundwater levels observed after 2020 are attributed to the final felling of 2019, which decreased transpiration, thereby increasing groundwater levels. While GWL, despite the considerable variance exists among observations at different locations, the simulations generally fell within the observed range and captured variations at both seasonal and dry-down time scales (Figure 4a). The  $R^2$  between average observed and simulated water table depths was  $0.7478$ , and the RMSE was  $-0.0908$  m (b). Therefore, the model reliably reproduced observed groundwater level (GWL) but with a clear, although relatively small, underestimation particularly manifesting apparent during winters. The model simulated lower groundwater levels during winter compared to the average among the four locations. However, this lower water table is not expected to significantly substantially impact soil  $\text{CO}_2$  emissions, as decomposition is impeded by low temperatures. Conversely, the model showed slightly higher groundwater levels during the driest summers, which is primarily influenced by evapotranspiration impeding decomposition.

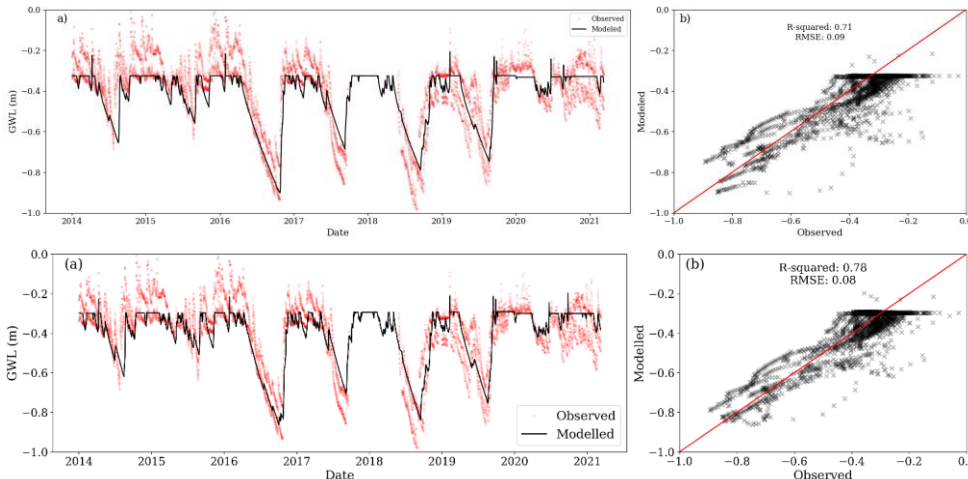
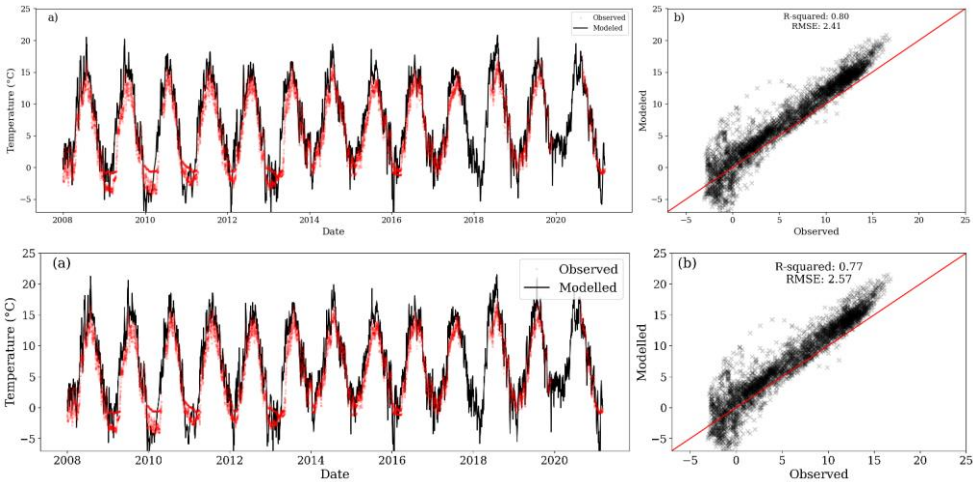


Figure 4. (a) Modelled height of GWL (black line) and observations (red dots) from 4 different locations within the site; negative values mean distance to the surface. (b) Correlation Relationship between the average of mean observed values GWL (averaged across locations) and modelled values GWL.

Formatted: Normal

360 Daily soil temperature from 2008 to 2021 exhibited low variability between locations. ~~Observed~~The observed mean annual soil temperature at 0.05 m depth was 5.57 °C, and the standard deviation was 5.4 °C. Simulated soil temperature in the first layer correlated strongly with the average observed temperature at 0.05 m among the three measurement locations ( $R^2$  of 0.8077, RSME of 2.4157 °C), as shown in Figure 5b. Similar comparisons of soil temperature at depths of 0.15 and 0.30 m are given in the appendix AAppendix C, with  $R^2$  values of  $\geq 0.7876$ . Simulated soil temperature showed slight but consistent overestimations over observations during spring and summer, which could lead to an overestimation of the decomposition temperature modifier function (Figure 5a).

365



370 **Figure 5.** (a) Modelled soil temperature for the first layer (black line) and observations at 0.05m depth (red dots) from 3 different locations within the site. (b) CorrelationRelationship between observed and modelled soil temperature values. During the period of comparison period, the first layer's centroid of the first layer was between 0.089077 m and 0.094m081 m.

375

### 3.1.2 Carbon fluxes

NEP measurements revealed that the site actingacted as a net sink of CO<sub>2</sub> in 2008 while still forested, transitioning to a CO<sub>2</sub> source in 2020 and 2021 after clear-cutting. While during 2008, the mean NEP was 0.55 gC m<sup>-2</sup>soil d<sup>-1</sup>; during 2020 and 2021, the mean NEP was -1.08 and -0.59 gC m<sup>-2</sup>soil d<sup>-1</sup>, respectively. Despite reproducing soil temperature and GWL reasonably well on a daily basis, the model failed to capture daily changes in NEP (Figure 6a). However, when aggregated to seasonal values, the model performed adequately. For fluxes aggregated over warm months (May, June, July, August, September and October) and cold months (November, December, January, February, March, and April), the model achieved

375

Formatted: Not Superscript/ Subscript

Formatted: Not Superscript/ Subscript

Formatted: Not Superscript/ Subscript

Formatted: Not Superscript/ Subscript

Formatted: Not Superscript/ Subscript

Formatted: Not Superscript/ Subscript

$R^2 = 0.8894$  and  $RMSE = 5540.8 \text{ gC m}^{-2} \text{ soil half-yr}^{-1}$  (Figure 6b). The model successfully captured the site transition from a carbon sink to a source. Observed annual NEP fluxes satisfactory. For 2008, 2020, and 2021 observations were 204, -396, and  $-216 \text{ gC m}^{-2} \text{ soil yr}^{-1}$ , respectively, while modelled the model estimated values were 152, 446 of 258, -282, and  $-383270 \text{ gC m}^{-2} \text{ soil yr}^{-1}$ , respectively.

380

385

390

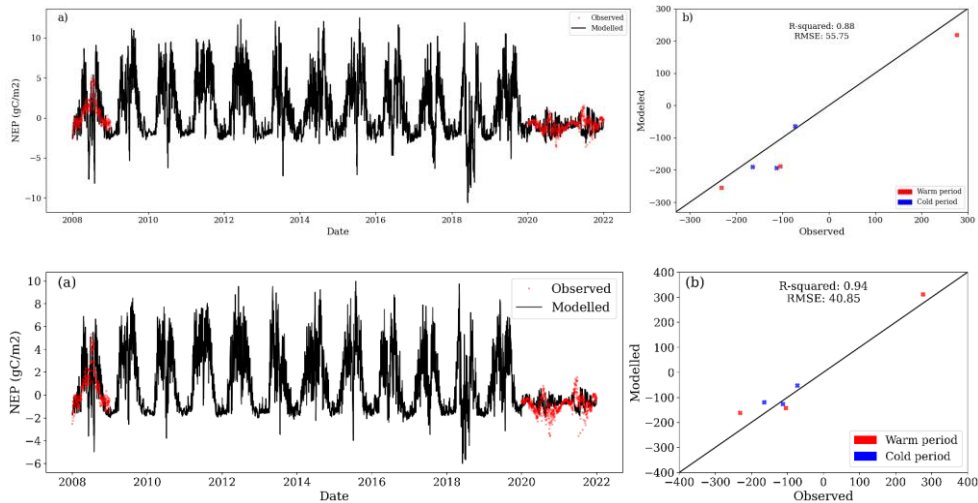


**Figure 6. (a) Modelled NEP net ecosystem productivity (black line) and observations (red dots). (b) Correlation Relationship between observed values and modelled net ecosystem productivity values. Values for correlation model evaluation correspond to the aggregation of fluxes into warm (May, June, July, August, September and October) and cold periods (November, December, January, February, March, and April) months of the year.**

### 3.2 Carbon exchange dynamics across system boundaries.

The simulated NCB and ICS were negative under all system boundary assumptions at the end of the second rotation, with the exception of the NBC at the ecosystem+HWP scale. Both metrics were strongly showed strong and similarly sensitivesimilar sensitivity to system boundaries (Table 1). The expansion of Expanding the system boundaries had a positive effect on positively influenced both the NCB and ICS, with the soil acting as a stronger source than showing the most negative values, followed by the ecosystem, which is in turn a stronger source than and then the ecosystem+HWP. Under the ecosystem+HWP boundaries, despite accumulating boundary, although the system accumulated more carbon than it loses lost

395

Formatted: Not Superscript/ Subscript

Formatted: Not Superscript/ Subscript

Formatted: Not Superscript/ Subscript



400

by the ~~end of the~~ simulation ~~end~~, the ICS ~~remains~~remained negative, indicating a potential persistent negative effect on climate over the same period.

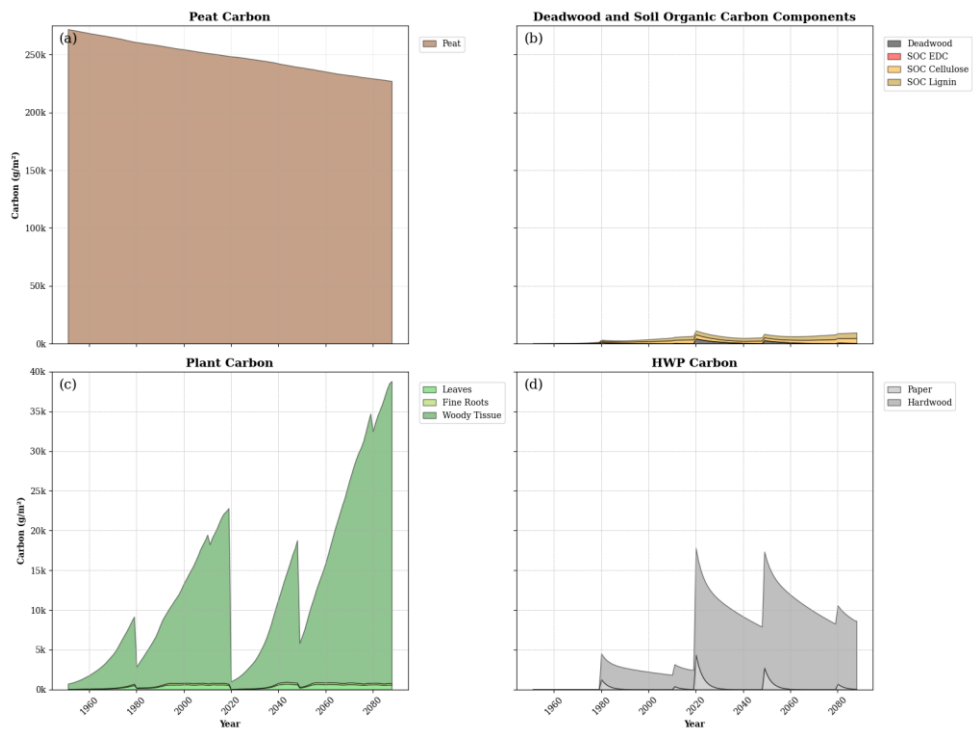
**Table 1. ~~Metries~~Net carbon balance (NCB) and integrated carbon storage (ICS) for the soil, ecosystem and ecosystem+HWP as system boundaries at the end of two forest ~~rotation~~rotations. HWP refers to harvested wood products.**

System boundaries	NCB (gc m <sup>-2</sup> <sub>soil</sub> )	ICS (gc yr m <sup>-2</sup> <sub>soil</sub> )
Soil	<del>-461733</del> <u>4897</u>	<del>-3.32.42</del> <u>×10<sup>6</sup></u>
Ecosystem	<del>-374662</del> <u>5249</u>	<del>-1.620</del> <u>×10<sup>6</sup></u>
Ecosystem+HWP	<del>10152307</del>	<del>-7.0×10<sup>5</sup></del> <u>.59×10<sup>6</sup></u>

405

The main carbon dynamics during the simulation are depicted in Figure 7. Within the soil, the peat ~~e~~ompartments~~stock~~ decreased with time. Peat losses were not compensated by ~~soils e~~ompartments~~soil stocks~~ associated with litter and biomass residues despite ~~significant~~large increments in those ~~e~~ompartments~~stocks~~ during the second rotation. The plant carbon ~~e~~ompartments~~stocks~~ were modulated by the cycle of forest management and environmental conditions, which increased plant carbon during the second rotation. HWP carbon ~~e~~ompartments~~significantly~~stocks substantially increased after 2019's clear ~~cut~~cutting.

410



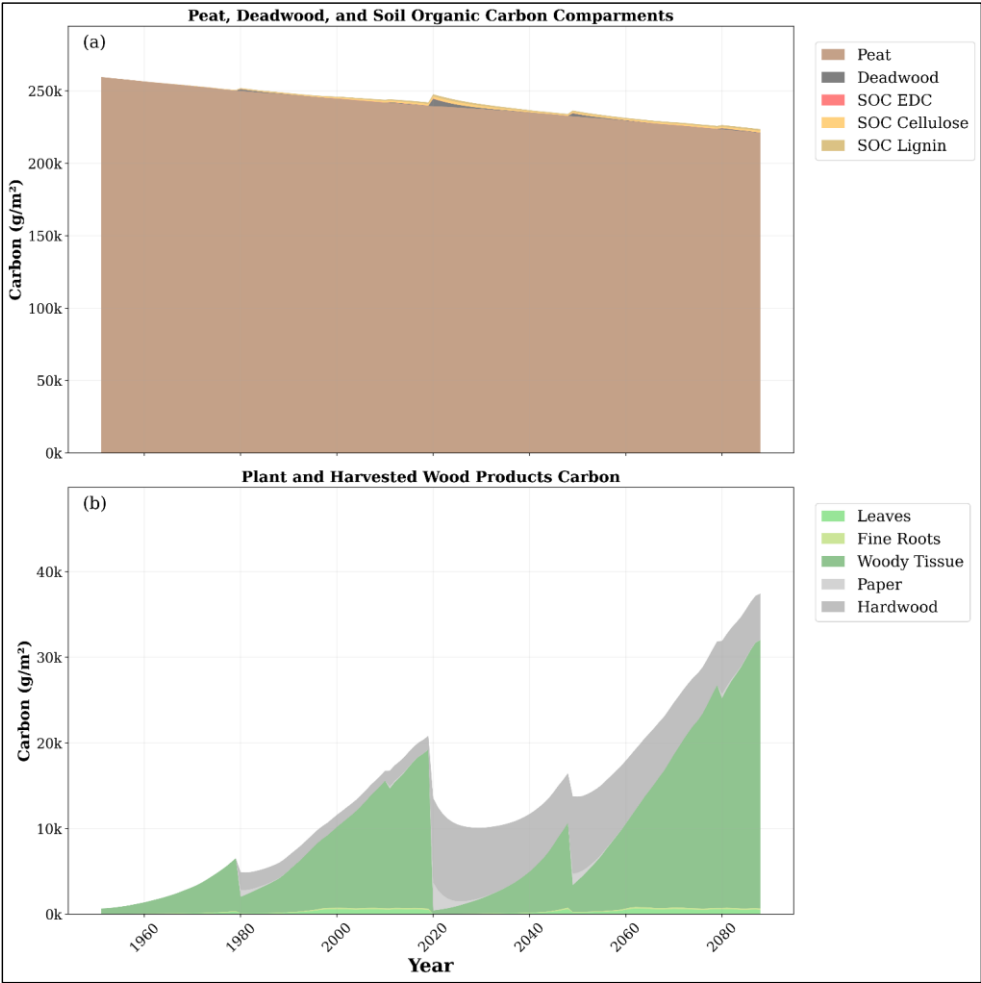


Figure 7. Temporal evolution of main carbon compartments stocks during the simulation. a) Carbon stocks in peat, deadwood, easily decomposed compounds, cellulose and lignin. b) Carbon stocks in leaves, fine roots, woody tissue (stem plus branches), and paper from harvested wood and hardwood products. Note the difference in scale of the y-axis between the upper plots and the lower plots.

### 3.2.1 Soil carbon dynamics

At the end of the ~~simulation~~ second rotation, for the soil system alone, the NCB was ~~-46173~~ gc34897  $\text{gC m}^{-2}_{\text{soil}}$ , while the ICS was ~~-3.32.42~~  $\times 10^6 \text{ gC yr m}^{-2}_{\text{soil}}$ . The NCB declined consistently over time, with the exception of transient recovery events associated with inputs of harvest residues ~~(b)~~ (Figure 8b). This reflects the persistent net loss of carbon despite the continuous inputs of litter to the soil ~~(a)~~ (Figure 8a). The ICS declined exponentially with time, as it accounts for the compounding effects of the emitted carbon residing in the atmosphere instead of in the soil or vegetation (Figure 8c).

The average annual carbon balance within the soil amounted to ~~-334252.8~~  $\text{gC m}^{-2}_{\text{soil yr}^{-1}}$ , showing virtually no significant differences between the first ~~rotation~~ (-330  $\text{gC m}^{-2}_{\text{soil yr}^{-1}}$  on average) and the second ~~rotation~~ (-338  $\text{gC m}^{-2}_{\text{soil yr}^{-1}}$  on average) rotations. Key inflows included litterfall and carbon transfers from deadwood, primarily dead stumps left after harvest. The site functioned as a small CH<sub>4</sub> sink, except during harvesting years when it became a slight CH<sub>4</sub> source. The most significant substantial outflow was through soil CO<sub>2</sub> emissions, whereas leached carbon (DOC, CH<sub>4</sub> in water and CO<sub>2</sub> in water) contributed only ~~10% and 415%~~ of total outflows respectively.

The annual balance was lowest at the onset of the forest rotation, due to low litter input and significant substantial soil CO<sub>2</sub> emissions from peat decomposition. For example, the annual soil balance was ~~-443330~~  $\text{gC m}^{-2}_{\text{soil yr}^{-1}}$  during the first five years of the first forest rotation, while it was ~~-309223~~  $\text{gC m}^{-2}_{\text{soil yr}^{-1}}$  during the last 8 years ~~of the first forest rotation~~. As the tree stand matured, the balance became less negative, occasionally turning positive during years with large litterfall inputs (e.g., ~~4283908~~  $\text{gC m}^{-2}_{\text{soil yr}^{-1}}$  as a result of the clear-cut cutting at the end of 2019).

Litter inputs ~~(not considering years of harvest)~~ notably increased during the second rotation (~~395144~~  $\text{gC m}^{-2}_{\text{soil yr}^{-1}}$ ) compared to the first rotation (~~238118~~  $\text{gC m}^{-2}_{\text{soil yr}^{-1}}$ ), attributed thanks to significantly higher larger tree biomass. Litterfall is heavily influenced by the size of the plant compartment they originate from. Leaf litter and root turnover were less influential increased as the forest matured stand aged due to its relation with woody litter assuming more importance biomass size. Litterfall from leaves and roots represented 81 % of the total litterfall, the rest being associated with branches and bark. Deadwood carbon transfer became particularly significant post-noteworthy in 2020 following clear-cut in 2019 cutting, compensating for low litter from small trees at the outset of the second rotation, becoming the primary input for the first ~~4418~~ years of this rotation. During the first rotation, deadwood transfer from dead stumps left after removals from management were was, on average ~~-36, 43~~  $\text{gC m}^{-2}_{\text{soil yr}^{-1}}$ , while during the second rotation were significantly, it was substantially higher, amounting to ~~407123~~  $\text{gC m}^{-2}_{\text{soil yr}^{-1}}$ .

CO<sub>2</sub> emissions from the soil were also higher during the second rotation (~~-856506~~  $\text{gC m}^{-2}_{\text{soil yr}^{-1}}$ ) compared to the first rotation (~~-586380~~  $\text{gC m}^{-2}_{\text{soil yr}^{-1}}$ ), partly due to increased carbon inputs from litter and deadwood, resulting in higher CO<sub>2</sub> emissions from the easily decomposed compounds (EDC), cellulose and lignin SOCSOM compartments. Nonetheless, emissions from peat decomposition remained the primary source of CO<sub>2</sub> throughout the simulation, with similar magnitudes between rotations. The decreasing availability of peat in the first three soil layers over time was offset by higher, resulting from reduced peat mass due to decomposition rates driven partially by, did not lead to lower decomposition fluxes because increasing soil

Formatted: Not Superscript/ Subscript

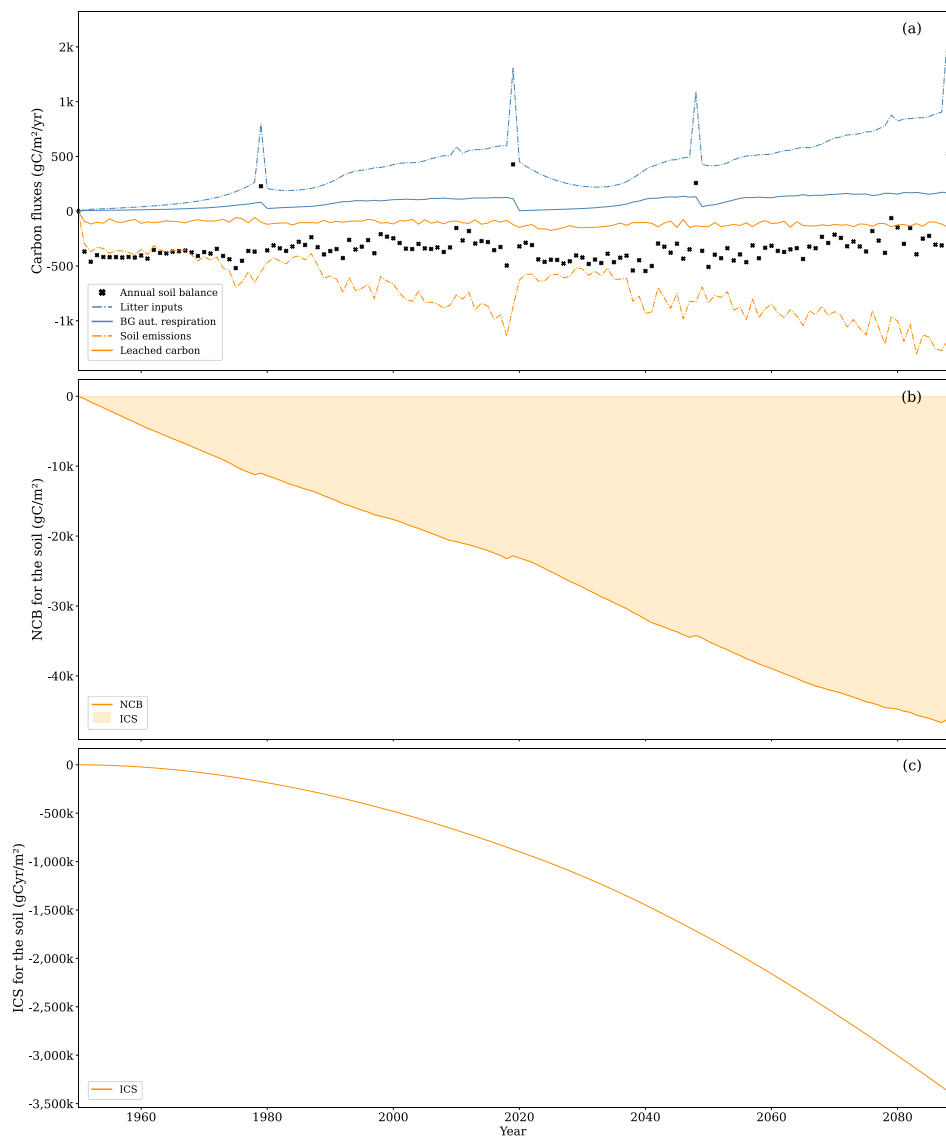
Formatted: Not Superscript/ Subscript

Formatted: Not Superscript/ Subscript

Formatted: Not Superscript/ Subscript

temperature: promoted decomposition. During the first rotation, the average peat decomposition rate ~~constant~~constants for the first, second and third soil ~~layer~~layers were 0.012, ~~0.01~~0.011 and ~~0.006~~0.007 yr<sup>-1</sup>, respectively; for the second rotation, the rate constants were 0.014, ~~0.01~~0.013 and ~~0.01~~0.011 yr<sup>-1</sup>. Additionally, peat available for aerobic decomposition from layers affected by ditch maintenance after the 2022 further supported persistent and high peat decomposition rates.

Formatted: Not Superscript/ Subscript



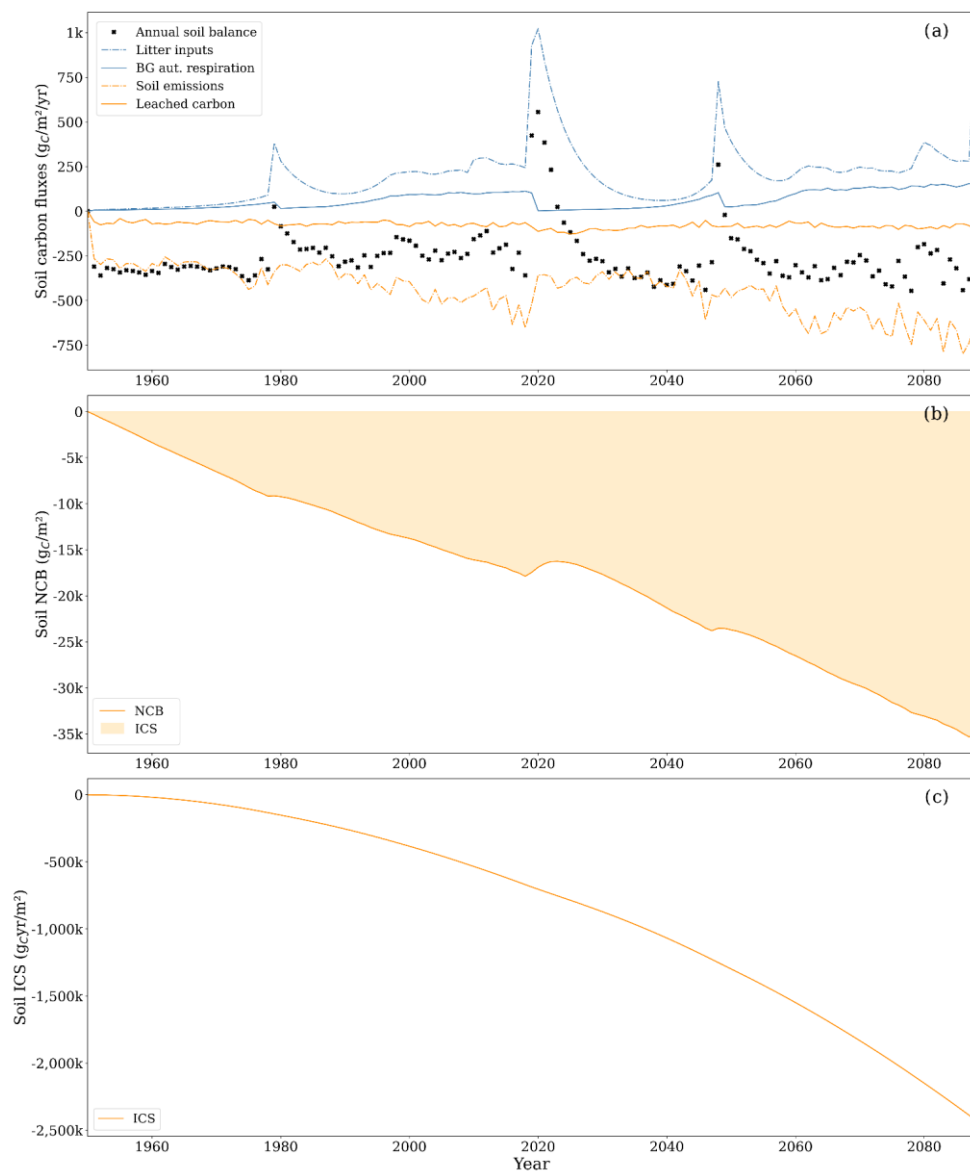




Figure 8. (a) Litterfall from trees and dead wood transfers to soil (dot-dashed blue line), autotrophic below-ground belowground respiration (solid blue line), CO<sub>2</sub> soil emissions from the soil (orange dot-dashed line) and leached carbon composed of CO<sub>2</sub> and DOC (orange solid line) and soil net yearly balance (black cross). Note that, for this boundary the soil system, autotrophic below-ground belowground respiration is an inflow of carbon to the soil. This increases soil CO<sub>2</sub> concentrations which in turn drive CO<sub>2</sub> soil emissions. Uptake of CH<sub>4</sub> and leached CH<sub>4</sub> were excluded from the graph as they comprised less than 1% of the total carbon flux. (b) NCB net carbon balance (solid line) during the period of analysis period and the ICS integrated carbon storage (shaded area). (c) ICS integrated carbon storage (solid line).

### 3.2.2 Ecosystem carbon dynamics

Focusing solely on the soil boundaries overlooks the primary mechanism through which afforested drained forested peatlands accumulate carbon, which is the living tissue of trees. Therefore, analyzing analysing carbon dynamics within the ecosystem boundaries becomes essential. Under these boundaries, both metrics reveal a system with a less negative carbon balance compared to the soil system defined by the soil boundaries, but still negative throughout the analysis period (Figure 9). By the end of the period of analysis second rotation, NCB was  $-3746625249 \text{ gC m}^{-2}_{\text{soil}}$ , while ICS was  $-1.620 \times 10^6 \text{ gC yr m}^{-2}_{\text{soil}}$ . Both metrics worsened became more negative from the end of the first rotation to the end of the second rotation.

Under these boundaries, the average annual carbon balance amounted to  $-274182 \text{ gC m}^{-2}_{\text{soil yr}^{-1}}$ . If the balance turns positive if harvest years are not accounted for the balance turns positive ( $198136 \text{ gC m}^{-2}_{\text{soil yr}^{-1}}$ ). Inflows are fundamentally exclusive from were primarily driven by the spruce stand GPP (i.e. the site was a small net sink of CH<sub>4</sub>), while). At the same time, the most significant important outflows included CO<sub>2</sub> emissions from the soil, aboveground autotrophic respiration, CO<sub>2</sub> emissions from the soil, and biomass harvesting, making up 37%, 32%, accounting for 35%, 34%, and 25% of total outflow, respectively. Aboveground respiration increased throughout the rotation because it is primarily controlled by plant biomass. On average, aboveground respiration accounted for 40% of GPP, with lower values during the initial years of the simulation (around 34% in the first nine years of the first rotation) and higher values as aboveground woody biomass became a higher proportion of the plant biomass (around 46% in the last nine years of the first rotation). Notably, changes between rotations were minimal. Soil CO<sub>2</sub> emissions followed a different trajectory. In the initial 9-year period, they represented 226% of GPP. However, as GPP increased faster than soil emissions, their relative contribution declined to 30% in the last 9 years of the first rotation. Similar values were observed in the subsequent rotation.

The temporal dynamics of flows explain the results for NCB and ICS. Early time trajectories. The rapid increase of GPP gradually offset early carbon losses during the rotation were gradually offset by the rapid growth of GPP. The tree biomass accumulates stores a fraction of the GPP, partially offsetting partially the accumulated soil losses until harvest removes tree biomass, sinking reducing the accumulated balance again. The metrics became more negative during the second rotation because sustained soil carbon losses were compounded with the soil carbon losses of the first rotation that were not compensated at the end of the first rotation.

During the second rotation, GPP notably increased to  $24021379 \text{ gC m}^{-2}_{\text{soil yr}^{-1}}$ , compared to  $4225889 \text{ gC m}^{-2}_{\text{soil yr}^{-1}}$  during the first rotation, so that the tree biomass at the end of the second rotation was 59% higher than in the first rotation. The increased photosynthetic rates are primarily attributed to the positive effect of higher atmospheric CO<sub>2</sub> concentration and higher

temperature embedded in the model formulation. This sets off a reinforcing loop where higher potential photosynthesis leads to increased biomass growth, resulting in a ~~high~~<sup>higher</sup> leaf area index (LAI) ~~that~~, further ~~boosts~~<sup>boosting</sup> photosynthesis.

495 ~~This~~<sup>However, this process</sup> can be ~~counter-balanced~~<sup>counterbalanced</sup> by several ~~processes, such as factors, including~~ self-shading, foliar nitrogen dilution and water limitation. While in both rotations, maximum LAI values were similar ~~being~~<sup>around</sup> ~~6.52~~<sup>6.52</sup> m<sup>2</sup><sub>leaf</sub> m<sup>-2</sup><sub>soil</sub>, the average LAI during the first rotation (~~3.32~~<sup>3.2</sup> m<sup>2</sup><sub>leaf</sub> m<sup>-2</sup><sub>soil</sub>) was ~~significantly~~<sup>significantly</sup> lower than the average value for the second rotation (~~4.53~~<sup>3.2</sup> m<sup>2</sup><sub>leaf</sub> m<sup>-2</sup><sub>soil</sub>), indicating ~~that~~ trees ~~achieving~~<sup>achieved</sup> maximum canopy faster in the second rotation. ~~Average~~<sup>The average</sup> foliar nitrogen content expressed as ~~a~~<sup>a</sup> percentage of leaf dry weight remained similar between

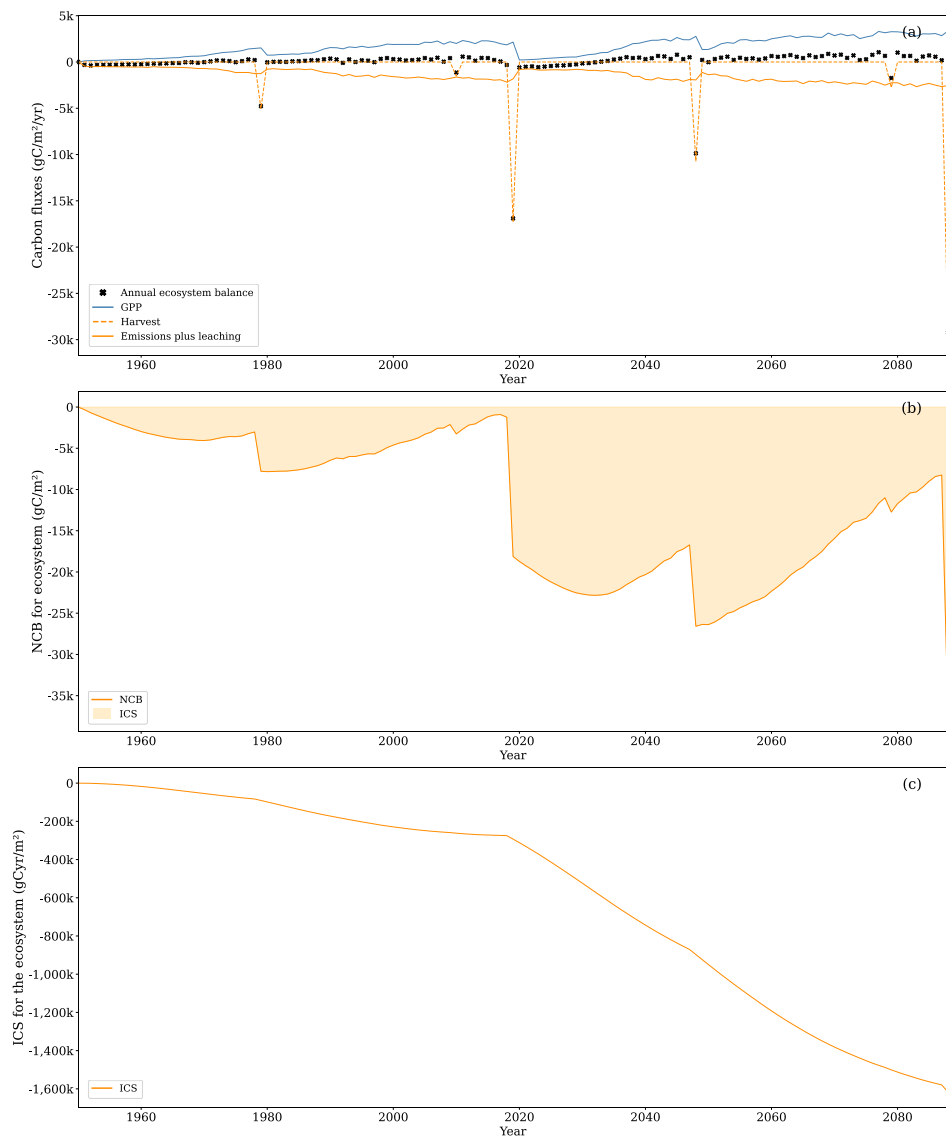
500 rotations (~~1.46~~<sup>52</sup>%). This was supported by consistently high nitrogen ~~mineralization, during~~<sup>mineralisation</sup>. ~~During~~ the first rotation, ~~the~~ average yearly nitrogen ~~mineralization~~<sup>mineralisation</sup> was ~~6.54~~<sup>7.02</sup> gN m<sup>-2</sup><sub>soil</sub> yr<sup>-1</sup>, while during the second rotation, ~~the~~ average yearly nitrogen ~~mineralization~~<sup>mineralisation</sup> was ~~8.56~~<sup>10.63</sup> gN m<sup>-2</sup><sub>soil</sub> yr<sup>-1</sup>. Similarly, water limitation was ~~not important~~<sup>unimportant</sup> in ~~neither of the rotations, either rotation, with~~ the ratio between actual plant water uptake and potential plant water uptake ~~was remaining at 0.97~~<sup>98</sup> for both. ~~However, in both rotations, some dry years, such as 2018, the ratio decreased to 0.91.~~

505 ~~ratio decreased to 0.91.~~

Formatted: Not Superscript/ Subscript

Formatted: Not Superscript/ Subscript

Formatted: Not Superscript/ Subscript



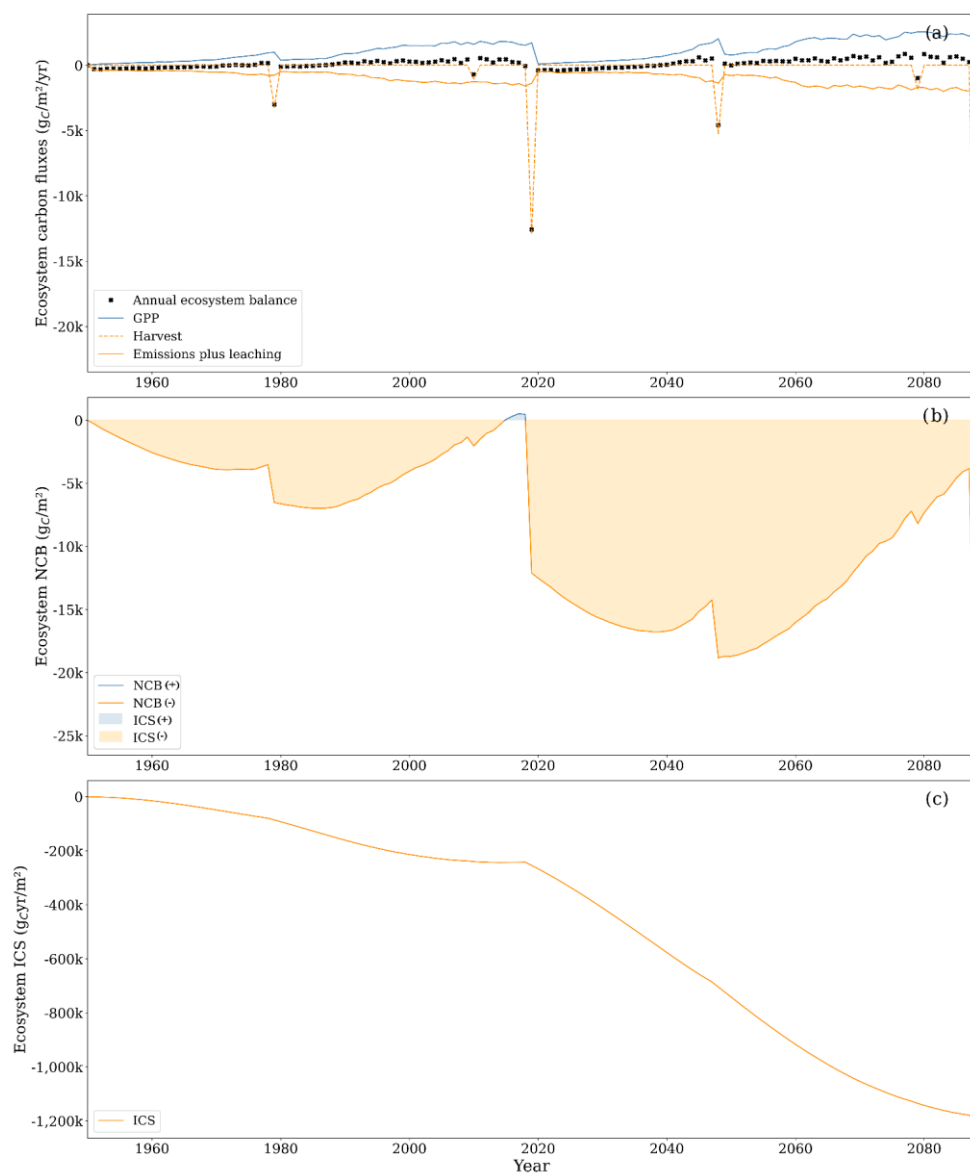
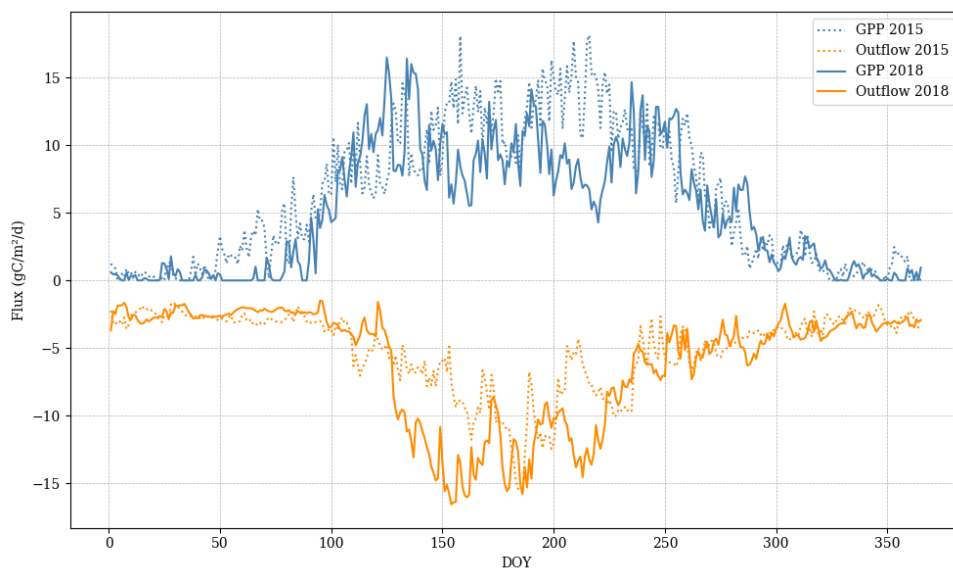
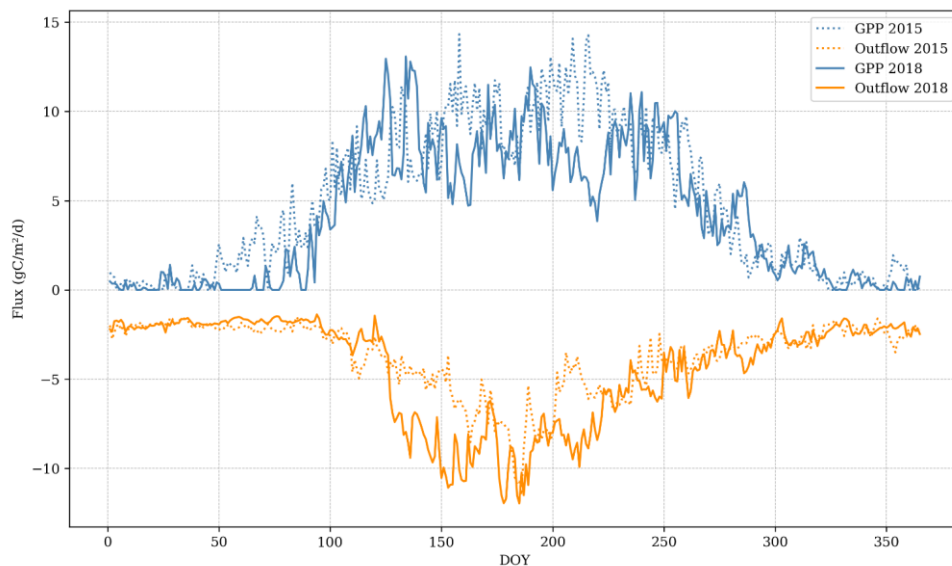


Figure 9. (a) Gross primary productivity (solid blue line), aboveground respiration, soil CO<sub>2</sub> emissions, and leached carbon composed of CO<sub>2</sub> and DOC (orange solid line), carbon outputs due to harvesting (orange dashed line), and ecosystem net yearly balance (black cross). Uptake of CH<sub>4</sub> and leached CH<sub>4</sub> were excluded from the graph as they comprised less than 1% of the total carbon flux. (b) Net carbon balance (solid line) and Integrated carbon storage (shaded area). (c) Integrated carbon storage (solid line)

In years without harvesting or extreme climatic conditions, GPP typically remains sufficiently high to offset ecosystem carbon losses, except during the initial years of a rotation years when LAI is less than 0.15 m<sup>2</sup> leaf m<sup>-2</sup> soil. Extreme climatic conditions can lead to a negative annual carbon balance, even in mature stands with high photosynthetic capacity (i.e. LAI > 65 m<sup>2</sup> leaf m<sup>-2</sup> soil). For instance, in 2018, when precipitation was 25% below the average for 2005-2019, the annual ecosystem balance was -38056 gC m<sup>-2</sup> soil yr<sup>-1</sup>. Conversely, in 2015, with precipitation 8% above the average, the balance was 341451 gC m<sup>-2</sup> soil yr<sup>-1</sup>. During 2018, GPP was 0.84% of 2015 GPP due to water limitations during the summer. Aboveground respiration remained high in 2018 despite lower growth due to plant maintenance respiration, suggesting that the size of the forest stand and temperature can amplify the negative effect on carbon fluxes of dry years. Soil emissions in 2018 were 1.3 times 137% of those of the 2015 emissions, suggesting that water limitation to decomposition in the upper soil layers is overridden by aerobic decomposition in deeper peat layers that remained moist (Figure 10).

Commented [DEC1]: Fix





**Figure 10.** Comparison between main ecosystem fluxes between a dry year (2018) and a normal year (2015). Outflow is comprised of soil CO<sub>2</sub> emissions, carbon-leached carbon and aboveground respiration.

During most-of the years, carbon accumulation in the plant compartment is more than the carbon lost by the soil compartments. Therefore, overlooking removals the removal of plant carbon by harvesting—amounting to 27.25% of the total carbon outflow from the ecosystem—could falsely suggest a carbon sink within the system. Across the two rotations, harvesting contributed to ana total outflow of -6727246534 gC m<sup>-2</sup> soil out of the 229598156550 gC m<sup>-2</sup> soil photosynthesized photosynthesised by the plants.

### 3.2.3 Ecosystem+HWP carbon dynamics

Under the ecosystem boundaries, carbon associated with harvested biomass is treated as an outflow, as if harvested carbon were in the form of CO<sub>2</sub> or DOC. However, harvested wood does not undergo rapid conversion to CO<sub>2</sub>. Consequently, the ideal boundaries for assessing effects on climate are those in which all outflows from the system ultimately leave as CO<sub>2</sub>.

Within the ecosystem+HWP system boundaries, harvested wood fate is tracked until its degradation into CO<sub>2</sub>, providing a comprehensive view long-term perspective on potential effects on climate. By the end of the period-of analysis second rotation, the NCB turned positive at 40452307 gC m<sup>-2</sup> soil, while ICS was large and negative at -7.0×10<sup>8</sup>.59×10<sup>6</sup> gC yr m<sup>-2</sup> soil (Figure 11). Both metrics declined by the end of the second rotation compared to the end of the first rotation, when NCB was 44762380 gC

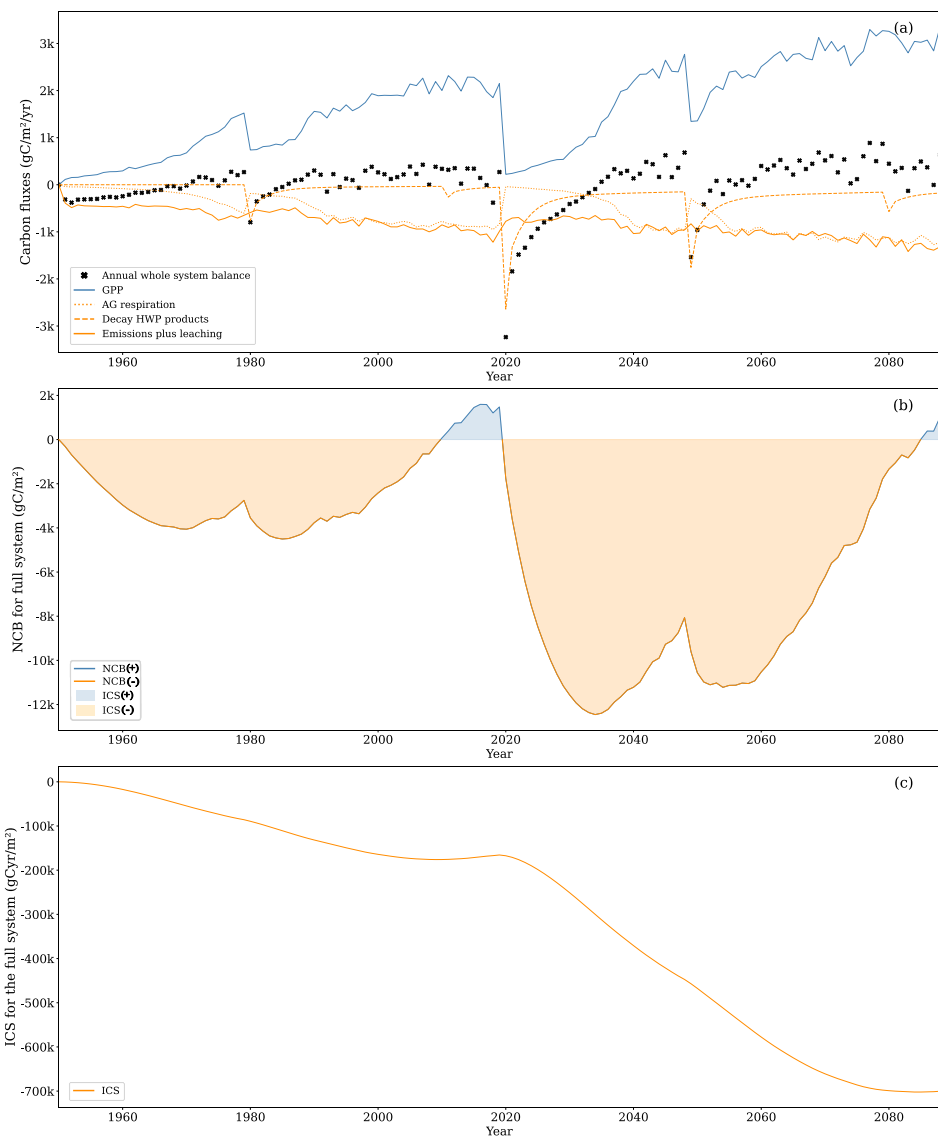
$\text{m}^2_{\text{soil}}$ , and ICS was  $-1.6 \times 10^5$  to  $0.17 \times 10^6$   $\text{gC yr m}^2_{\text{soil}}$ . This trend can be attributed to the compensation of early soil carbon losses by forest growth that is not completely cancelled by harvesting due to the slow decay of some harvested carbon. The capacity of wood products to hold carbon for some time resulted in a positive carbon balance by the end of each rotation. However, the ICS displays a negative trend because the initial losses are substantial, and later compensation is neither sufficient nor sustained long enough to counterbalance the extent and duration of the negative carbon balance under these system boundaries.

In the ecosystem+HWP system boundaries, the primary inflow of carbon was GPP, with negligible soil uptake of  $\text{CH}_4$ . The most significant important outflows were, in order of importance, aboveground respiration, soil carbon emissions, above-ground respiration, degradation decay of harvested wood products and soil carbon leaching. Above-ground respiration increased during the rotation because is largely controlled by plant biomass. On average, above-ground respiration accounted for 36% of GPP, with lower values during the initial years of the simulation (around 29% in the first five years) and higher values as above-ground woody biomass became a higher proportion of the plant biomass (around 42% in the last five years of the first rotation). Notably, changes between rotations were minimal.

Throughout each rotation, soil carbon losses decreased by higher inputs of fresh litter from larger plant biomass. In the initial 10-year period, soil losses represented 220% of GPP, gradually decreasing to 50% in the final 5 years of the first rotation. Similar values were obtained for the subsequent rotation. Harvested wood degradation peaks during the decay of harvested wood products peaks in the year of harvest, directly proportional to the harvested biomass, with temporal dynamics independent of GPP fluctuations. During the second rotation, the total carbon loss from decaying harvested wood degradation was 5 products accounted for 8% of total GPP. Carbon These outflows from harvested wood increased during in the second rotation because carbon decay from the harvested wood during due to the 2019 clear-cut event were significant for cutting, which transferred a substantial amount of carbon to harvested wood products. In the first 20 years of rotation, carbon outflows from decaying harvested wood products were approximately 10% of aboveground respiration and soil  $\text{CO}_2$  emissions, while in the second rotation, this proportion increased to 40%. The total outflow from decaying harvested wood products in the second rotation was 16,269  $\text{gC m}^2_{\text{soil}}$ , with half occurring between 2020 and 2043.

Clear Although accounting for the slow decay of harvested wood products moderates the impact of clear-cutting changed on the net carbon balance drastically, this intense harvesting process still caused a drastic shift at the end of the first rotation. From 1986 until 2019, the annual rate of change of the NCB is was positive (175233  $\text{gC m}^2_{\text{soil yr}^{-1}}$ ), which led to a positive NCB since year from 2010 until 2019. During that period, the ICS negative trend slowed down. The effect of clear-cut Clear-cutting in 2019 quickly reduced the NCB, which experienced a strong negative rate of change during the first 10 years of the second forest rotation (-1263960  $\text{gC m}^2_{\text{soil yr}^{-1}}$ ). The NCB was projected to become slightly positive only until 2085 in 2083. The year after the clear-cut cutting, GPP would be was reduced by 99.5% compared to the previous year, while soil emissions would remained high while. The decay of HWP would be 10 times larger than harvested wood products exceeded GPP for the first eight years of the GPP second rotation.





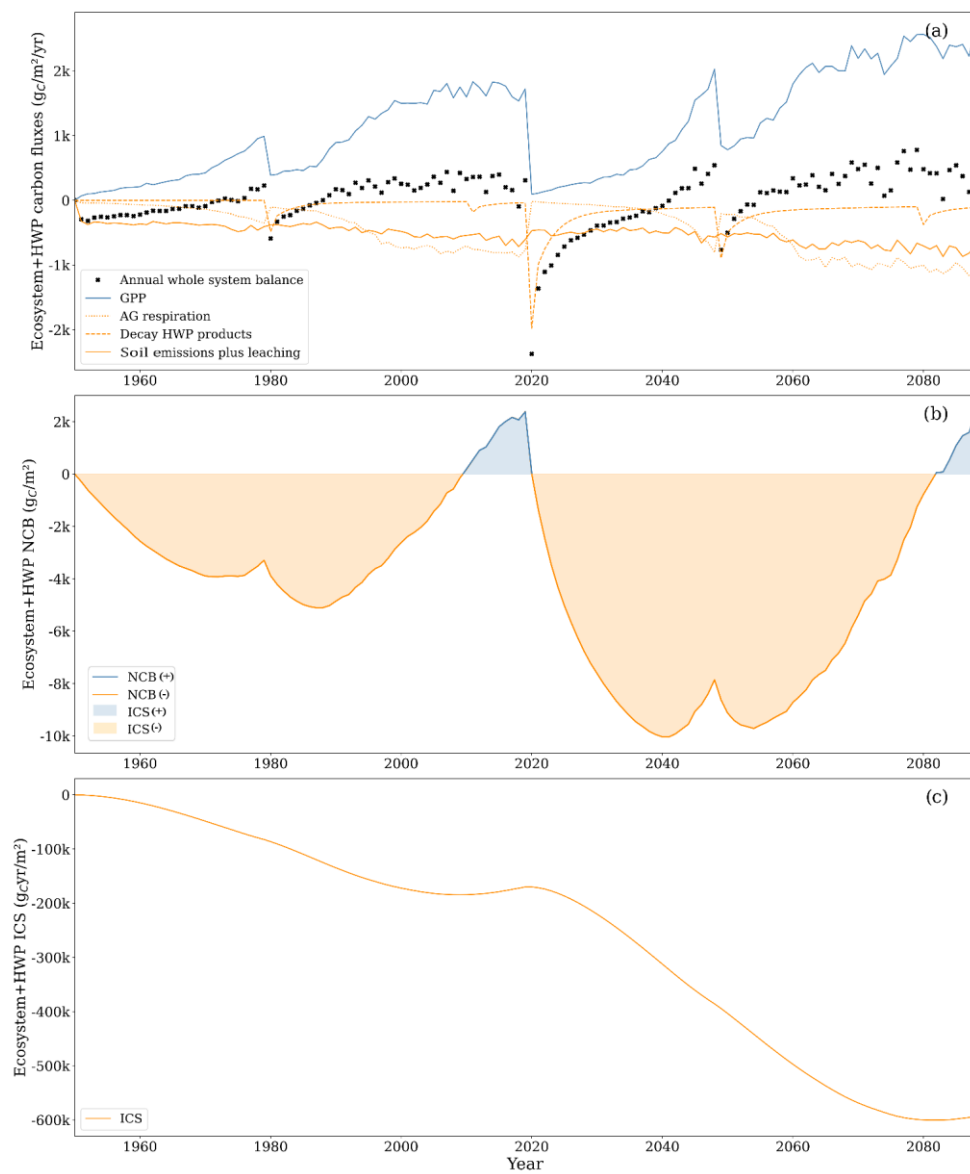


Figure 11. (a) Gross primary productivity (solid blue line), aboveground respiration (orange dotted line), soil carbon ~~loses~~ losses comprising soil CO<sub>2</sub> emissions and leached carbon composed of CO<sub>2</sub> and DOC (orange solid line) ~~and~~, CO<sub>2</sub> from decay of harvested wood products made out of wood harvesting (orange dashed line), and ecosystem + harvested wood products net yearly balance (black cross). Uptake of CH<sub>4</sub> and leached CH<sub>4</sub> were excluded from the graph as they comprised less than 1% of the total carbon flux. (b) NCB net carbon balance (solid line) and ICS integrated carbon storage (shaded area). (c) ICS integrated carbon storage (solid line).

## 4 Discussion

### 4.1 On the representativeness of simulated carbon dynamics and the abiotic context

Site conditions can substantially influence the magnitude of carbon fluxes in northern drained forested peatlands. Therefore, soil emission factors for this land category are classified based on nutrient availability, climate conditions, and drainage level (Jauhainen et al., 2023; Wilson et al., 2016).

In our simulated peatland, nutrient conditions are primarily determined by an initial soil organic matter C:N ratio of 21. Under these conditions, sites are often classified as Herb-rich type (Ojanen et al., 2010) or eutropic (Minkinen et al., 2020). drastically change the magnitude of carbon fluxes in northern afforested drained peatlands; therefore, soil emission factors for this land category are classified according to climatic and nutrient categories (Wilson et al., 2016). Average modelled soil temperature of 7.0°C for the period of 1990 to 2020 is similar to those found in cool temperate or hemiboreal sites in the south of Sweden or The average modelled soil temperature of 7.0°C from 1990 to 2020 aligns with values observed in cool temperate or hemiboreal sites in southern Sweden and Estonia (Minkinen et al., 2007; Ranniku et al., 2024). Simulated water table is representative of a well-drained site with functional ditches. During

Regarding drainage, during the first rotation, the average mean annual GWL was -0.43 m—similar comparable to other well- drained afforested forested peatlands (Leppä et al., 2020; Maljanen et al., 2012; Menberu et al., 2016). Spatial variability of GWL within one site can be high, as illustrated by differences across locations within the site. This is often associated with the effect of distance from the ditch network (Laudon & Maher Hasselquist, 2023). Reported mean annual GWL values are often around -0.3 m and -0.5 m for distances from the ditch of 5 m and 15 m. Slightly lower values were observed toward the end of the rotation due to peat subsidence. Reported mean annual GWL values typically range between -0.3 m and -0.5 m at distances of 5 m and 15 m from the ditch, respectively (Haapalehto et al., 2014). Groundwater level tends to increase during the rotation in afforested drained peatlands due the combined effects of subsidence and ditch degradation on drainage (He et al., 2016). In our model formulation this behaviour arises because decomposition leads to shrinkage in layers of peat where there is water lateral flow. In our simulations, GWL had slightly lower values during the first 34 years of the rotation (-0.45 m) than during the last 35 years (-0.42 m). Simulated site nutrient conditions—soil organic matter C:N ratio of 21—are similar to other very nutrient rich drained peatlands. Under these conditions Water table fluctuations simulated by ForSAFE-Peat reflect those of a well-drained site with functional ditches. sites are often classified as Herb-rich type (Ojanen et al., 2010) or eutropic (Minkinen et al., 2020).

610 ~~Given the site~~ Based on these characteristics, it is understandable our simulated site can be classified as nutrient-rich and well-  
drained, with a climate that falls between boreal and temperate regions. This classification helps explain why our estimates of  
litterfall minus soil  $\text{CO}_2$  emissions carbon balance during the first rotation ( $-341 \pm 252 \text{ gC m}^{-2} \text{ yr}^{-1}$ ) are similar to those found in  
afforested drained forested peatlands previously used for agriculture at the same latitude in cool temperate regions ( $-256 \text{ gC m}^{-2} \text{ yr}^{-1}$ ) by a metanalysis of field-based observations (Jauhiainen et al., 2023). ~~Despite our values being more negative, they are~~  
615 still well within the variability reported (Jauhiainen et al., 2023; Jovani-Sancho et al., 2021; Lazdins et al., 2024). Comparable  
observations for soil  $\text{CO}_2$  emissions are mostly limited to dark chamber measurement that did not remove litter and that include  
belowground autotrophic respiration. As an example, Arnold et al., (2005) estimated soil  $\text{CO}_2$  emissions at  $-388 \text{ gC m}^{-2} \text{ yr}^{-1}$  for  
an afforested drained peatland with a 50-year-old Norway spruce stand. In contrast, our estimation for the first rotation, when  
our spruce stand was between 45 and 55 years old, was  $-716 \text{ gC m}^{-2} \text{ yr}^{-1}$ . While these sites shared some similarities, such as the  
620 grown tree species, the site described by Arnold et al., (2005) had lower nitrogen availability (C:N ratio of 28), lower carbon  
content (bulk density of  $0.17 \text{ g cm}^{-3}$ ), and a higher water table ( $-0.27 \text{ m}$ ). Overall, the literature exhibits significant variability,  
and our estimations tend to fall on the higher end of this range. For instance, Ball et al. (2007) estimated soil emissions at  $-610$   
 $\text{gC m}^{-2} \text{ yr}^{-1}$  for a 30-year-old Spruce stand, compared to our estimation of  $-651 \text{ gC m}^{-2} \text{ yr}^{-1}$  for a 29-year-old stand in 1978,  
before thinning in 1979.

625 . These values are at the higher end of estimations for the more general category of drained forested peatlands in northern  
latitudes, but they are still well within the variability reported (Jauhiainen et al., 2023; Jovani-Sancho et al., 2021).  
It is important to note that our study site was actively afforested, as it was initially an open fen. While peatlands with substantial  
tree cover are relatively rare in the UK, spruce and pine mires are more common in Sweden and even more prevalent in Finland  
(Laine et al., 2006). Peatlands without prior tree cover before drainage are likely to have higher soil water saturation levels  
630 than those with substantial tree cover (Beaulne et al., 2021). On peatlands with substantial tree cover, carbon accumulation in  
the upper soil layers is likely more dependent on stabilisation mechanisms occurring under aerobic conditions (Kilpeläinen et  
al., 2023). In contrast, carbon in peatlands without substantial tree cover is more likely stabilised by anoxic conditions, making  
it more sensitive to water table drawdown. Such nuances in carbon dynamics are often lost in the broad categories used to  
account for carbon in these land-use systems.

635 Comparable observations for soil  $\text{CO}_2$  emissions to our simulations are mostly limited to dark chamber measurements that did  
not remove litter and include belowground autotrophic respiration. For example, Arnold et al. (2005) estimated soil  $\text{CO}_2$   
emissions at  $-392 \text{ gC m}^{-2} \text{ yr}^{-1}$  for a drained forested peatland with a 50-year-old Norway spruce stand. In contrast, our estimation  
for the first rotation, when our spruce stand was between 45 and 55 years old, was  $-442 \text{ gC m}^{-2} \text{ yr}^{-1}$ . While these sites shared  
some similarities, such as the grown tree species, the site described by Arnold et al. (2005) had lower nitrogen availability  
640 (C:N ratio of 28), lower carbon content (soil carbon density of  $0.07 \text{ gC cm}^{-3} \text{ soil}$ ), and a higher water table ( $-0.27 \text{ m}$ ). Overall,  
data in the literature exhibits large variability, and our estimations tend to fall on the higher end of this range.

DOC leaching is often assumed to be a less important component of the soil carbon outflux than soil  $\text{CO}_2$  emissions and is not  
often reported. Wilson et al. (2016) estimated  $-30 \text{ gC m}^{-2} \text{ yr}^{-1}$  for temperate ~~afforested~~ drained forested peatlands, but the lack

of data did not allow ~~to for~~ separate fluxes by nutrient status. We calculated an average of ~~-7234~~  $\text{gC m}^{-2} \text{yr}^{-1}$  during the first rotation. ~~However, our~~ Our ratio of soil  $\text{CO}_2$  emissions to DOC exports of ~~0.1409 during the first rotation~~ was similar to the 0.12 of Wilson et al. (2016). Interestingly, the ratio between leached DOC and GPP in our study (~~0.0508~~) was around the ~~average ratio of 0.04~~ higher end (range: 0.002 to 0.08) estimated for Swedish watersheds by Manzoni et al. (2018). Notably, these ratios in our study were much higher during the first years of rotation due to the effect of drainage and the absence of ~~significant~~ substantial photosynthetic activity, highlighting the impacts of processes such as clear ~~cuts~~ cutting (Gundale et al., 2024).

~~Estimations of annual litter inputs in 35-year-old spruce stands under a long-term soil warming fertilization study in northern Sweden by Leppälampi-Kujansuu et al. (2014) align closely with our simulated values ( $264 \text{ gC m}^{-2} \text{yr}^{-1}$ ) for our stand prior to the 1979 thinning, when it was 28 years old. Correspondingly, similar litter input values ( $212\text{--}356 \text{ gC m}^{-2} \text{yr}^{-1}$ ) have been reported for young Norway spruce stands (~30 years old) in nutrient-rich conditions slightly north of our site (Blaško et al., 2022). Furthermore, literature findings regarding Norway spruce stands in~~ Soil carbon losses, in the form of  $\text{CO}_2$  emissions and DOC leaching, can be offset by litter inputs. Litterfall rates in Norway spruce exhibit considerable variability and are highly sensitive to nutrient status (Kleja et al., 2008). In nutrient-rich conditions, measured litterfall rates for Norway spruce have been estimated at 150 and  $301 \text{ gC m}^{-2} \text{yr}^{-1}$  (Blaško et al., 2022), which are similar to our simulated average of  $198 \text{ gC m}^{-2} \text{yr}^{-1}$  when the LAI exceeded  $2.0 \text{ m}^2_{\text{leaf}} \text{m}^{-2}_{\text{soil}}$ . Our average litter production rate for the first rotation ( $118 \text{ gC m}^{-2} \text{yr}^{-1}$ ) was lower than the  $219 \text{ gC m}^{-2} \text{yr}^{-1}$  reported in a modelling study by Kleja et al. (2008), which simulated nutrient-rich conditions at a site in southern Sweden using the COUP model. However, values measured in a Norway spruce stand in Sweden (Hansson et al., 2013), Finland (Hilli, 2013), Estonia (Uri et al., 2017), and Latvia (Bārdule et al., 2021) demonstrate comparability with our estimates. However, our study may have overestimated litter inputs from woody tissue and foliage, as indicated by measurements conducted by Hilli (2013); are comparable to our estimates.

The magnitude of litterfall is closely tied to plant biomass, which increases with GPP fluxes (Ojanen et al., 2014). ~~GPP observations are often derived from net ecosystem production (NEP) measurements using partitioning assumptions. For instance, Mamkin et al. (2023) reported a five-year average GPP of  $1494 \text{ gC m}^{-2} \text{yr}^{-1}$  for old Norway spruce on peat in Russia with an average LAI of  $3.5 \text{ m}^2_{\text{leaf}} \text{m}^{-2}_{\text{soil}}$ , comparable to our estimation of  $1432 \text{ gC m}^{-2} \text{yr}^{-1}$  for LAI values ranging between 3.2 and  $3.9 \text{ m}^2_{\text{leaf}} \text{m}^{-2}_{\text{soil}}$  during the first rotation. Additionally, Korkiakoski et al. (2023) estimated a five-year average GPP of  $1406 \text{ gC m}^{-2} \text{yr}^{-1}$  in a nutrient-rich peatland afforested with spruce and pine in the south of Finland, with an LAI slightly above  $2 \text{ m}^2_{\text{leaf}} \text{m}^{-2}_{\text{soil}}$  determined using remote sensing. Our GPP estimations for similar LAI values were around  $1128 \text{ gC m}^{-2} \text{yr}^{-1}$ . Moreover, simulated GPP values during the first two years after clear-cutting ( $221$  and  $241 \text{ gC m}^{-2} \text{yr}^{-1}$ ) closely align with those reported by Korkiakoski et al. (2019) for a nutrient-rich drained peatland post clear-cut ( $175$  and  $298 \text{ gC m}^{-2} \text{yr}^{-1}$ ). Using partitioning assumptions, GPP observations are often derived from net ecosystem production (NEP) measurements. For instance, Mamkin et al. (2023) reported a five-year average GPP of  $1494 \text{ gC m}^{-2} \text{yr}^{-1}$  for old Norway spruce on peat in Russia with an average LAI of  $3.5 \text{ m}^2_{\text{leaf}} \text{m}^{-2}_{\text{soil}}$ , comparable to our estimation of  $1295 \text{ gC m}^{-2} \text{yr}^{-1}$  for a similar LAI value ( $3.56 \text{ m}^2_{\text{leaf}} \text{m}^{-2}_{\text{soil}}$ ) during the first rotation. Additionally, Korkiakoski et al. (2023) estimated a five-year average GPP of  $1406 \text{ gC m}^{-2} \text{yr}^{-1}$~~

in a nutrient-rich drained forested peatland with spruce and pine in the south of Finland, with an LAI slightly above  $2 \text{ m}^2_{\text{leaf}} \text{ m}^{-2}_{\text{soil}}$  determined using remote sensing. Our GPP estimations for similar LAI values were around  $1128 \text{ gC m}^{-2} \text{ yr}^{-1}$ . However, simulated GPP values during the first two years after clear-cutting ( $93$  and  $110 \text{ gC m}^{-2} \text{ yr}^{-1}$ ) were lower than those reported by Korkiakoski et al. (2019) for a nutrient-rich drained peatland following clear-cutting ( $179$  and  $301 \text{ gC m}^{-2} \text{ yr}^{-1}$ ). This discrepancy highlights the importance of non-tree vegetation in sustaining GPP after clear-cutting, which was captured by Korkiakoski et al. (2019) but not accounted for in our model.

4.2 On model GPP in the second rotation increased by 64%, driven by higher temperatures and elevated atmospheric  $\text{CO}_2$  concentrations under a context of nitrogen and water availability. Increased photosynthetic activity in Norway spruce under free air  $\text{CO}_2$  enrichment experiment has been documented. Bader et al. (2016) reported an increase of 73% in the photosynthetic rate of the upper-canopy shoots with an atmospheric  $\text{CO}_2$  concentration increase of 150 ppm. Similarly, Sigurdsson et al. (2002) observed a 53% increase in the rate of light-saturated photosynthesis under high nitrogen availability with an atmospheric  $\text{CO}_2$  concentration increase of 350 ppm.

Under a reasonable abiotic regime, defined by realistic water table depth and soil temperature, the decomposition representation used in ForSAFE-Peat—similar to those of models like ORCHIDEE and LPJ—produces credible estimates of peat losses. Additionally, the PnET default parameterisation for carbon assimilation, respiration, and litterfall, combined with the calibrated respiring wood fraction, yields realistic tree biomass accumulation. These results align closely with values reported in the literature for similar systems, supporting the model's ability to simulate carbon dynamics in drained forested peatlands under comparable conditions.

#### 4.2 Model limitations:

The model demonstrates a capability to reproduce ForSAFE-peat reproduced GWL and soil temperature observations with reasonable accuracy. However, it simulates lower GWL during winter, likely due to its omission of the effects of freezing effects on water flow. Additionally, the underestimation of GWL during the driest summer periods may be attributed to inaccuracies in simulating Evaporation and transpiration, which are influenced by root distribution and plant or excessively fast lateral water use efficiency—parameters that were not calibrated flow associated with drainage. The model's simplistic approach used to simulate drainage may also fail to capture critical hydrological dynamics, such as anisotropic hydraulic conductivity, ditch geometry, or water-induced soil volume changes—through peat swelling.

Regarding temperature, the model tends to overestimate spring and summer temperatures. This overestimation may result from a lower GWL at the onset of spring compared to observations, which reduces heat capacity and possibly heat conductivity. Furthermore, the simplistic upper boundary condition of discrepancy might arise from the model, along with the lack of not accounting for heat fluxes associated with soil surface evapotranspiration and the temperature modulation by trees, contributes to this discrepancy, mainly through evapotranspiration latent heat fluxes and canopy shading.

710 Despite these ~~simplifications~~shortcomings, the model provides a reasonable abiotic context for assessing carbon dynamics. It is essential, however, to evaluate the limitations ~~on carbon of the representation on of the model formulation~~carbon cycle and its implications in ~~the our results from this study~~. The model followed commonly used formulations for peat soils (Kleinen et al., 2012; Qiu et al., 2018), where peat is defined as a conceptual compartment with unspecified chemistry, that decomposes ~~linearly according to a following first-order exponential decay, with~~ rate constants modified by environmental conditions.

715 LimitationsEven though this description provides reasonable carbon dynamics at yearly and decadal time scales, limitations within this representation might explain why ~~the model did not represent~~ daily NEP fluxes ~~were not well-represented by the model~~. Firstly, in ~~the~~ current model structure, ~~optimum moisture conditions for~~ decomposition ~~rates~~ increase slowly with moisture content until field capacity, ~~however the but this~~ response ~~might could~~ be faster in peat soils (Rewcastle et al., 2020; Ľupek et al., 2023). Furthermore, the complex redox chain that controls decomposition in peat soils is simplified by a function

720 ~~that only considers~~considering water content. In reality, ~~non-saturated even unsaturated~~ conditions can lead to ~~limited aerobic conditions~~anoxia if ~~strong intense~~ decomposition depletes oxygen (Fan et al., 2014). Conversely, fully saturated conditions might not ~~result in form~~ methane ~~formation~~ if electron acceptors like nitrate or sulphate are available (Cui et al., 2024; Reddy & DeLaune, 2008).

~~The linear rate constants~~A description of decomposition ~~are not adequate based on first-order exponential decay is inadequate~~ to capture non-linear responses such as respiration pulses at rewetting due to combined microbial reactivation and changes in substrate availability (Manzoni et al., 2020) or priming effects associated with substrate quality. ~~Is well-established that phenolic~~Phenolic compounds can downregulate enzymes responsible for decomposing other carbon compounds, resulting in negative priming effects that inhibit overall decomposition (Freeman et al., 2001). Conversely, ~~the~~ allocation of labile carbon through roots can stimulate decomposer activity in coniferous-dominated soils (Jílková et al., 2022; Leppälampi-Kujansuu et al., 2014; Li et al., 2020). ~~In, though in~~ nutrient-rich sites like the one simulated, this ~~effect~~ may be less ~~significant~~important

730 ~~than in nutrient-limited conditions, however sites. While these contrasting priming effects have been reported,~~ the overall response of soil organic carbon decomposition to root exudates in coniferous ~~forest~~forests remains unclear (Gundale et al., 2024). Interestingly, measurements of carbon ~~sinks~~accumulation in ~~soils from afforested~~drained forested peatlands ~~have often come from been conducted in~~ nutrient-poor sites ~~and using chamber methods that with root trenching, which~~ do not

735 ~~consider account for~~ the effect of labile carbon allocated by roots ~~in on~~ heterotrophic respiration (Hermans et al., 2022).

~~The~~Generally, a model that explicitly represents the interactions between organic carbon substrates and microbial communities is desirable for exploring priming effects and the consequences of increased precipitation variability. However, in the context of this study, we suspect that the additional uncertainties in the microbial process parameterisation would decrease the benefit of a microbial-explicit model. Besides increasing process representation, peat decomposition models based on first-order

740 kinetics could benefit from representing SOM as measurable pools, especially if field-based decomposition data for chemically distinct, measurable SOM pools, coupled with field-based carbon balance data, become more readily available.

Similarly, the way plant carbon is simulated has certain limitations. For instance, carbon allocation of carbon within plant compartments follows a ~~simplifies~~simplified scheme where the allocation to root tissue is not directly influenced by in which

Field Code Changed

Formatted: English (United States)

Formatted: English (United States)



water and nutrient availability. ~~It is well recognized that the proportion of carbon allocated to roots do not directly influence root allocation. Yet, plants can increase when plants need carbon allocation to roots to enhance their resource acquisition (Prescott et al., 2020). Additionally, the model maximizes foliage growth based on light conditions, but wood growth does not affect light availability. The way wood is represented in the model implies some limitations. During the later stages of a forest rotation, when stand biomass is substantial, the model predicts that woody litter is the main form of carbon input to the soil. Additionally, wood respiration is identified as a primary source of CO<sub>2</sub>. The current model version does not differentiate between sapwood and hardwood and assumes that wood turnover is proportional to wood biomass. In reality, growth is represented by new sapwood, which is the fraction that respire, while sapwood gradually transforms into hardwood, and only a small portion of the bark ends up in the soil (Ogle & Pacala, 2009; Ukonmaanaho et al., 2008). The model also simplifies wood dynamics. It assumes a fixed proportion between sapwood and heartwood, considering sapwood the only wood fraction that respire, while woody litterfall is modelled as a fixed proportion of total wood mass. For this reason, as trees age and wood tissue comprise a larger fraction of total plant biomass, both wood respiration and woody litterfall increase. In reality, the proportion between sapwood and heartwood is dynamic, changing as trees grow. Wood growth originates in the sapwood, which gradually transforms into heartwood. This gradual change in the proportion between sapwood and hardwood affects both respiration rates and litterfall patterns, a process not captured by the model's fixed allocation scheme. The model could be improved with a more dynamic representation of wood dynamics. However, the allocation rates and respiration costs of sapwood are not well understood and are difficult to measure, posing challenges for accurately parameterizingparameterising a model given their importance in tree carbon dynamics (Metzler et al., 2024).~~

~~Furthermore, the current model formulation implies a very strong response to elevated atmospheric CO<sub>2</sub> values that lead to very high photosynthetic rate during the second rotation causing twice the growth compared to the first rotation. This might be an overestimation based on values derived from CO<sub>2</sub> enrichment experiments (Bader et al., 2016; Uddling & Wallin, 2012). However, is still useful to analyse the system under very high carbon uptake values during the second rotation. Currently the model does not account for understory vegetation, in nutrient rich afforested peatlands, grasses and mosses can dominate photosynthetic activity during the first 10 years of forest rotation (He et al., 2016). This exclusion may result in the model underestimating GPP and litter inputs during early years. Nonetheless, as evidenced by the measured data in this study, drained conditions during the initial years of forest rotation are likely characterized by significant carbon losses due to elevated decomposition of soil organic matter, especially when coupled with DNM (Korkiakoski et al., 2019; Palviainen et al., 2022). Furthermore, GHG emissions from ditches are also sensitive to DNM (Evans et al., 2016; Nieminen et al., 2018). Lastly, we assumed that a constant fraction of wood is allocated to HWP compartments. Our assumption that 65% of harvested wood has been used in other studies (Kasimir et al., 2018), however this fraction varies based on wood quality~~

~~Furthermore, the current model formulation suggests a strong response to rising atmospheric CO<sub>2</sub> concentration, leading to notably high photosynthetic rates during the second rotation. This effect is driven by enhanced carbon assimilation and water~~

use efficiency, resulting in greater growth. These responses have been both theorised and observed in forests exposed to elevated CO<sub>2</sub> levels (Donohue et al., 2017; Sigurdsson et al., 2013). However, there is uncertainty about the magnitude of these effects due to long-term acclimation and interactions with other environmental factors, such as increasing ozone concentrations or changes in vapour pressure deficit driven by higher temperatures, which may offset or alter the benefits of elevated CO<sub>2</sub> (Gustafson et al., 2018).

Despite uncertainties, it is still useful to analyse the system under conditions of very high carbon uptake by trees, especially because the model neglects understory vegetation and its contribution to carbon assimilation. It has been estimated that in nutrient-rich, drained forested peatlands, grasses and mosses can dominate photosynthetic activity during the first 10 years of a forest rotation (He et al., 2016). This exclusion may result in the model underestimating GPP and litter inputs during the early years. Nonetheless, as evidenced by the measurements in this study, drained conditions during the initial years of forest rotation are characterised by much larger carbon losses due to elevated decomposition of soil organic matter, particularly when ditch network maintenance lowers the groundwater level (Korkiakoski et al., 2019; Palviainen et al., 2022) and stimulates aerobic decomposition (Evans et al., 2016; Nieminen et al., 2018).

Lastly, we assumed that a constant fraction of wood is allocated to HWP compartments. Our assumption is that 65% of harvested wood has been used in other studies (Kasimir et al., 2018). However, this fraction varies based on wood quality (Jonsson et al., 2018; Profft et al., 2009).

The current model formulation of carbon dynamics, based on common representations embedded in other models, generally provides a reasonable platform for analysing peatland systems despite certain limitations. While this contribution focuses on a drained forested site, the model structure is flexible and applicable to other conditions, such as waterlogged soils (not drained) and natural vegetation, including grasses and mosses, provided appropriate parameterisation of the vegetation submodel is implemented.

#### 4.3 On-system boundaries and metrics of carbon exchange

Assessing the net carbon exchanges (~~—and thus, by extension, the potential effect on climate—~~ impacts ~~—in afforested drained forested~~ peatlands is ~~intrinsically/inherently~~ dependent on the delineation of system boundaries and the ~~chosen/selected~~ evaluation metrics. This study ~~argues/proposes~~ that the ~~optimal/most effective~~ system boundaries ~~to assess/for assessing~~ long-term carbon exchanges ~~encompass all~~ are those where inflows as atmospheric CO<sub>2</sub> take the form of gaseous carbon uptake from the atmosphere and all outflows as CO<sub>2</sub> released ~~into~~ take the form of gaseous carbon releases to the atmosphere ~~—referred to here as—~~. The ecosystem+HWP<sup>22</sup> boundary used in this study serves as an approximation of this premise.

Within these boundaries, different metrics can offer divergent perspectives on climatic effects. Our analysis reveals that ~~towards the end of rotations,~~ the system accumulated more carbon than it released ~~—towards the end of rotations,~~ resulting in a positive NCB. However, NCB fails to account for the temporal dynamics of carbon accumulation within the system (Sierra, 2024)(Muñoz et al., 2024). A small, constant carbon gain over time can yield the same NCB as carbon dynamics

810 ~~characterized~~characterised by substantial initial losses followed by substantial later gains within the analysis period. However, these scenarios may not have equivalent effects on climate.

The influence of carbon dioxide on climate change, manifested through alterations in the planetary energy balance, depends on both the atmospheric CO<sub>2</sub> concentration and the residence time of each CO<sub>2</sub> molecule in the atmosphere (Joos et al., 2013). Consequently, when a system exhibits substantial carbon losses throughout the analysis period, only compensated towards the

815 end, the interval during which accumulated losses exceeded accumulated gains can be interpreted as a period of negative effect on the climate, despite an eventual positive effect (i.e., accumulated losses became less than accumulated gains). Furthermore, designating the end of the rotation as the final point of the analysis period introduces bias, as any accumulated carbon in biomass is relatively quickly lost upon harvesting.

This temporal information is captured by ICS, providing a more comprehensive assessment of the climatic impact of specific carbon dynamics within a system. This is especially important in drained peatlands where high carbon losses ~~in at~~ the beginning

820 ~~of a rotation~~ are compensated only towards ~~theits~~ end-of-the-rotation, leading to negative ICS. A substantial proportion of Fennoscandian drained ~~afforestedforested~~ peatlands are approaching stand maturity, prompting imminent management decisions (Lehtonen et al., 2023). A very negative but improving ICS ~~mightmay~~ be a representative pattern for these systems; ~~therefore, avoiding clear-cutting is crucial to prevent declines in this metric. It is thuswould be~~ important to assess the

825 ~~effecteffects~~ of different management strategies ~~given this legacy effect on climate. ContinuousICS, especially those that do not rely on clear-cutting, such as continuous~~ forest cover (CCF) has been proposed as an alternative to manage current drained afforested peatlands (Laudon & Maher Hasselquist, 2023).

~~However, a limitation of the ICS is that it only considers carbon fluxes. N<sub>2</sub>O fluxes are substantial in nutrient-rich drained peatlands, and considering CH<sub>4</sub> emissions is necessary to assess rewetting as a management strategy (Jauhiainen et al., 2023; Kasimir et al., 2018). A metric that integrates all GHG through time considering the legacy effect of drainage is necessary to assess the management options to improve effects on climate from afforested drained peatlands. Given the relatively fast release of carbon from HWP after harvesting and potentially high release of potent CH<sub>4</sub> during initial years of successful rewetting. While the ICS provides valuable information for evaluating the climatic impact of a specific trajectory of carbon exchange, as demonstrated in the present study, it does not account for the varying warming effects associated with different types of carbon compounds exchanged (e.g., methane emissions under waterlogged conditions). Therefore, to assess alternative land use scenarios for forested drained peatlands, such as rewetting, a metric that incorporates both temporal dynamics and the warming effects of all GHGs, such as cumulative radiative forcing (Murphy & Ravishankara, 2018), would be ideal. Given the relatively fast release of carbon from HWP after harvesting and the potentially high release of the potent greenhouse gas CH<sub>4</sub> during the initial years of successful rewetting (Escobar et al., 2022), the effect on climate of combining clear-cut-cutting~~

830 ~~and rewetting could take a long time~~ to be compensated (Ojanen & Minkinen, 2020). ▲

835

840

Formatted: Not Strikethrough

## 5 Conclusions

The ForSAFE-peat model was able to realistically reproduce soil abiotic (temperature and GWL) conditions and annual net ecosystem productivity at the drained and forested, nutrient-rich peatland at Skogaryd. ~~However, while the model could capture the observed net ecosystem exchange reliably, it was unable to reproduce the daily observations of carbon exchange in Southern Sweden.~~ The model predicted a substantial increase in biomass growth in the future following higher temperatures and atmospheric CO<sub>2</sub> concentration, supported by higher precipitation and nitrogen mineralisation, and shows that even such a large increase in photosynthesis may not compensate for the large carbon losses caused by drainage-enhanced decomposition from drained peat-soil. The results underline the importance of choosing the choice-of-the appropriate system boundary considered-in-for carbon budget estimates, and argues argue for a more holistic budget accounting for the ecosystem and the fate of the harvested biomass. The study also shows how accounting for the temporal dimension of the carbon budget of a managed forest site can give fundamentally different estimates of the potential effect on climate warming. The study contrasts the NCB, which only focuses on book-keeping balances over a given period, with the more integrative ICS, which accounts for the time CO<sub>2</sub> resides in the atmosphere, and indicates that the former may give misleading estimates of climatic implications. Based on the testing at Skogaryd, we show that even if the nutrient-rich site may appear as a net sink at the end of a forest rotation, its legacy effect on ~~the~~ climate can remain negative given that much of the captured carbon was released in the atmosphere longer than it was fixed at the site, thereby producing a warming effect. We finally argue for a pragmatic adoption of dynamic modelling in estimating the effects of forest management on climate warming despite their limitation as illustrated here, and underline the importance of broader ecosystem boundaries in these estimates as well as more representative indicators accounting for the temporal aspect of forest management on carbon residence.

## Appendix A: Model sensitivity analysis

Model sensitivity analysis was performed to test the effect of uncertainty on the initial nutrient status and future precipitation level (Figure A1). A total of 9 scenarios were created based on a combination of 3 initial CN ratio scenarios and 3 precipitation scenarios for the years 2020-2088. The sensitivity analysis reveals that both water and nutrient availability regulate carbon dynamics. The higher NCB at the end of the simulation is associated with the high-nutrient, high-precipitation scenario. In comparison, the lower NCB is associated with the low-nutrient low-precipitation scenario. The NCB difference between these two scenarios was 9180 gC m<sup>-2</sup>. Given that the ICS is the time-integrated NCB, the sensitivity analysis also reveals negative ICS across all scenarios.

Formatted: Subscript

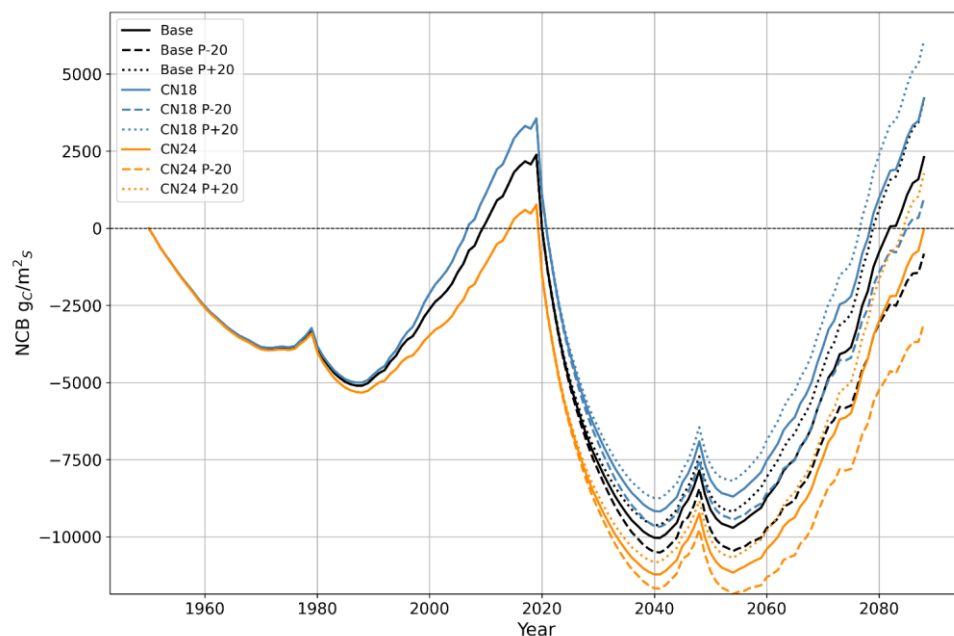


**Figure A1. Sensitivity analysis of net carbon balance (NCB) for the Ecosystem+HWP boundary: Each colour represents a different C:N ratio, and each line style indicates a specific future precipitation scenario. The black lines correspond to a C:N ratio of 21, used in the primary simulation of this study (Base). Blue lines represent a C:N ratio of 18, while orange lines represent a C:N ratio of 24. Dotted lines indicate a scenario with 20% higher precipitation from 2020–2088 compared to the main simulation, while dashed lines represent a scenario with 20% lower precipitation during the same period.**

Within the model formulation, nitrogen and water directly influence carbon dynamics, as illustrated in Figure A1. Nutrient content in soil organic matter regulates the nitrogen mineralisation rate, which controls nitrogen uptake by trees. This uptake determines leaf nitrogen content, thereby influencing GPP. Simultaneously, precipitation regulates soil water content, affecting both water uptake by trees and decomposition rates through soil water content.

Higher nutrient availability primarily impacts the net carbon balance (NCB) by increasing GPP. However, water availability may become a limiting factor as nutrient conditions improve and growth accelerates. In contrast, higher precipitation benefits the NCB by enhancing GPP and reducing decomposition rates. These causal relationships explain why similar NCB values were observed at the end of the simulation for two scenarios: one combining a C:N ratio of 21 with 20% higher precipitation

885 (dotted black line in Figure A1) and another with a C:N ratio of 18 (solid blue line in Figure A1) under precipitation levels  
matching the main simulation.

**Appendix B: Soil physical changes**

890 Peat soils are highly dynamic, undergoing expansion and contraction driven by changes in their carbon and water balance. To  
capture this behaviour, the model incorporates a dynamic volume approach, in which the soil organic matter balance directly  
controls each soil layer's thickness. This mechanism allows the model to simulate interactions between carbon accumulation,  
decomposition, and water content, which collectively influence the structure of peat soils over time. Figure B1 illustrates these  
dynamics, highlighting the simulated thickness and bulk density changes throughout the analysis period.

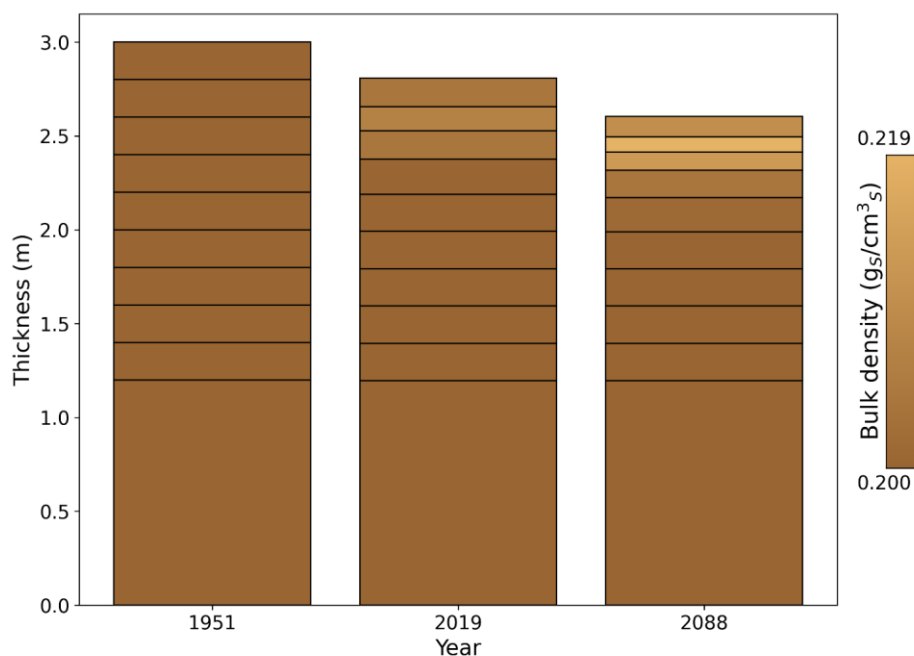


**Figure B1.** Simulated peat soil thickness and bulk density at three key time points: 1951, 2019, and 2088. The year 1951 marks the beginning of the simulation, coinciding with the establishment of tree planting. By 2019, the first forest rotation is completed, followed by a second rotation ending in 2088. The y-axis represents the cumulative thickness of the peat soil layers, with the total thickness shown for each year. The colour gradient indicates the soil bulk density ( $g_{\text{soil}}/\text{cm}^3_{\text{soil}}$ ) of the soil layers, where lighter shades represent higher bulk density values.

Simulated changes in the soil profile followed observed patterns in drained peatlands. The overall thickness of the soil profile decreased due to a sustained negative carbon balance at the soil level, driven by higher peat decomposition rates compared to litter inputs. The reduction in thickness occurred in layers above the groundwater level, where aerobic decomposition dominates. Changes in bulk density were only noticeable in these upper layers. In the first layer, changes were less pronounced than in the second layer, as most litter inputs were concentrated in the first layer.

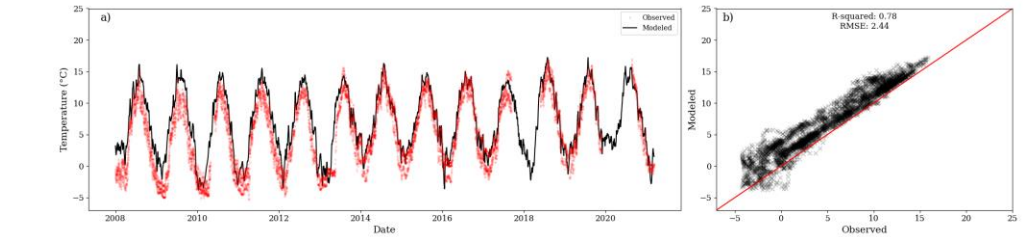
From 1951 to 2088, the model projected a total subsidence of 0.395 m, primarily driven by carbon losses in the upper four layers of the peat profile. This result aligns closely with the estimated subsidence of 0.357 m in peatlands used for forestry over 136 years of drainage, as calculated using an empirically based model derived from a meta-analysis of centennial-scale shifts in the hydrophysical properties of peat induced by drainage (Liu et al., 2020).

Regarding changes in bulk density, the rate of change in the upper three layers was approximately  $1.30 \times 10^4 \text{ g}_{\text{soil}} \text{ m}^{-3} \text{ soil yr}^{-1}$ , which is lower than the  $5.60 \times 10^4 \text{ g}_{\text{soil}} \text{ m}^{-3} \text{ soil yr}^{-1}$  estimated by Liu et al. (2020) for drained forested peatlands. Despite differences between the original bulk density of those sites ( $0.07 \text{ g}_{\text{soil}} \text{ cm}^{-3} \text{ soil}$ ) and our initial bulk density ( $0.20 \text{ g}_{\text{soil}} \text{ cm}^{-3} \text{ soil}$ ), the underestimation of the rate of change is likely due to ForSAFE-Peat not accounting for the collapse of soil pore space under drained conditions. According to Liu et al. (2020), most changes in bulk density occur within the first 30 years of drainage, likely due to the collapse of macropores shortly after drainage (Silins & Rothwell, 1998).

In ForSAFE-Peat, bulk density changes are driven by the ratio of mineral soil content to organic soil content, which fluctuates as organic soil content increases or decreases. If organic soil content decreases, the fraction associated with mineral soil content increases, meaning the average particle density also increases, as minerals are denser than organic matter. If the average particle density increases while porosity remains constant, bulk density increases.

**Appendix C: Further model performance evaluation.**

Further model evaluation ~~of model~~ was performed against temperature for depths of 0.15 m and 0.30 m. The modelled temperature at 0.20 m is was similar to the observed temperature at 0.15m. ~~However, slight overestimations are persistent~~ (Figure A1).





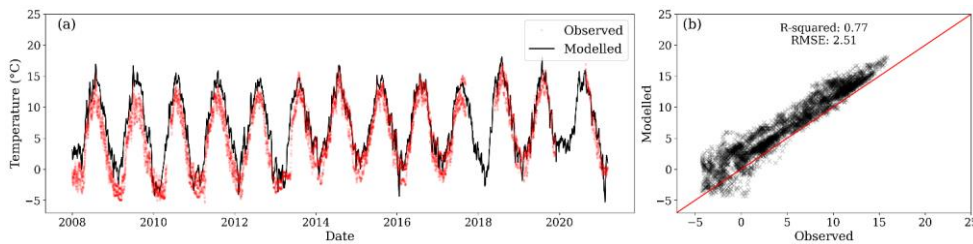


**Figure A1C1.** (a) Modelled temperature for the second layer (black line) and observations at 0.15m depth (red dots) from three locations. (b) Correlation Relationship between observed and modelled values. During the period of comparison, the centroid of the first layer was between 0.215m-223m and 0.22m-225m

Equally, the modelled temperature for a depth of 0.38m was similar to the observed temperature at 0.30m (Figure A2). However, a slight overestimation is persistent at this depth.

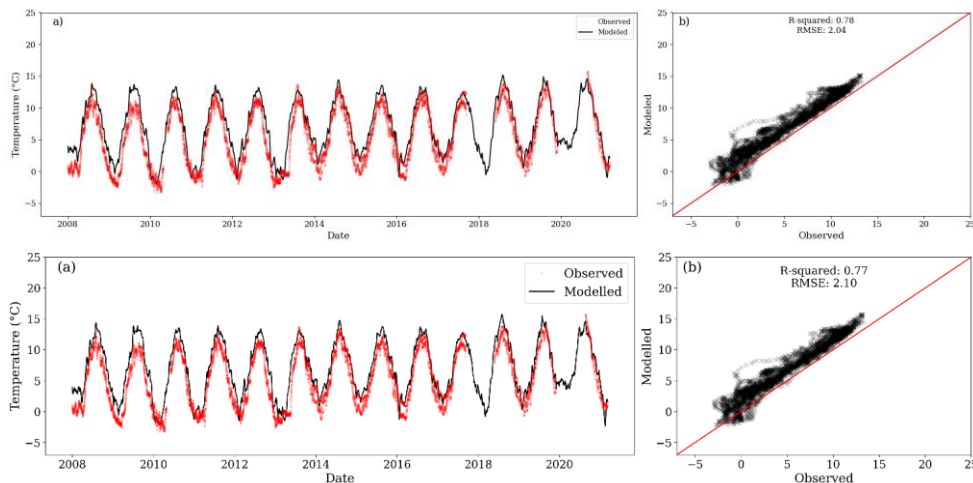


**Figure A2.** (a) Modelled temperature for the third layer (black line) and observations at 0.30m depth (red dots) from three locations. (b) Correlation Relationship between observed and modelled values. During the period of comparison, the centroid of the first layer was between 0.39m-372m and 0.38m-364m

**Appendix B: Carbon dynamics**

The net plant carbon balance, expressed as the net primary productivity minus litterfall, is usually higher than the soil carbon losses and actively compensate for peat decomposition in normal years Figure B1. This explains the negative effect generated by harvesting.

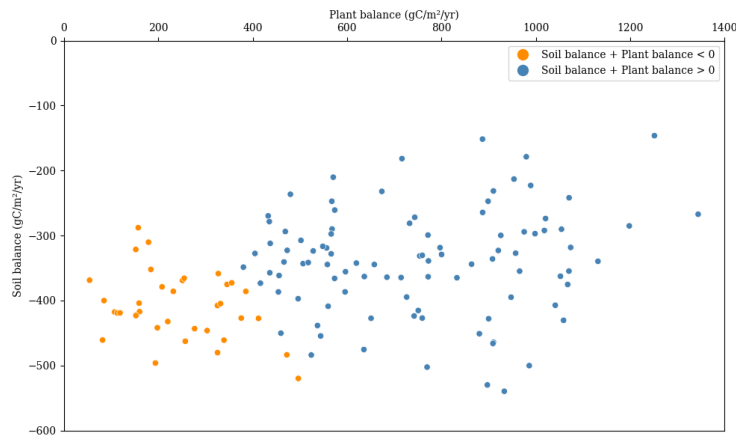


**Figure B1. Relation between net primary productivity and soil balance. In orange values when the net between soil balance and NPP is negative and blue values when is positive.**

**Code availability:**

The original model code of ForSAFE-Peat is written in Fortran 90 and is freely available upon request to the model developers (see contact details above) with the intent to support new user in the initial stage of their work with the ForSAFE model.

**Data availability:**

Field measurement data used to validate the model, along with and yearly model outputs of carbon fluxes encompassing the full extent of the simulation, are publicly available at [10.5281/zenodo.13626716](https://doi.org/10.5281/zenodo.13626716) and [10.5281/zenodo.13629155](https://doi.org/10.5281/zenodo.13629155)

**Author contribution:**

DE led the study. DE, SB and SM conceptualized the study. DE and SB conducted the formal analysis and investigation. SM and JT assisted in the formal analysis and investigation. All the authors discussed the results together. DE

wrote the original draft of the paper and produced the figures, with feedback from SB and SM. All authors reviewed and  
955 commented on the original draft of the paper and its revisions.

**Competing interest:**

The authors declare that they have no conflict of interest

**References**

Aber, J. D., & Federer, C. A. (1992). A ~~generalized~~generalised, lumped-parameter model of photosynthesis, evapotranspiration  
960 and net primary production in temperate and boreal forest ecosystems. *Oecologia*, 92(4), 463–474.  
<https://doi.org/10.1007/BF00317837>

~~Aber, J. D., Ollinger, S. V., & Driscoll, C. T. (1997). Modeling nitrogen saturation in forest ecosystems in response to land  
use and atmospheric deposition. *Ecological Modelling*, 101(1), 61–78. [https://doi.org/10.1016/S0304-3800\(97\)01953-4](https://doi.org/10.1016/S0304-3800(97)01953-4)~~

965 ~~Aber, J. D., Reich, P. B., & Goulden, M. L. (1996). Extrapolating leaf CO2 exchange to the canopy: A generalized model of  
forest photosynthesis compared with measurements by eddy correlation. *Oecologia*, 106(2), 257–265.  
<https://doi.org/10.1007/BF00328606>~~

Arnold, K. V., Weslien, P., Nilsson, M., Svensson, B. H., & Klemedtsson, L. (2005). Fluxes of CO2, CH4 and N2O from  
drained coniferous forests on organic soils. *Forest Ecology and Management*, 210(1), 239–254.  
970 <https://doi.org/10.1016/j.foreco.2005.02.031>

~~Bader, M. K. F., Mildner, M., Baumann, C., Leuzinger, S., & Körner, C. (2016). Photosynthetic enhancement and diurnal  
stem and soil carbon fluxes in a mature Norway spruce stand under elevated CO2. *Environmental and Experimental  
Botany*, 124, 110–119. <https://doi.org/10.1016/j.envexpbot.2015.12.005>~~

Bärdale, A., Petaja, G., Butlers, A., Purviņa, D., & Lazdiņš, A. (2021). Estimation of litter input in hemiboreal forests with  
975 drained organic soils for improvement of GHG inventories. *Baltic Forestry*, 27(2), Article 2.  
<https://doi.org/10.46490/BF534>

Beaulne, J., Garneau, M., Magnan, G., & Boucher, É. (2021). Peat deposits store more carbon than trees in forested peatlands of the boreal biome. *Scientific Reports*, 11(1), 2657. <https://doi.org/10.1038/s41598-021-82004-x>

Belyazid, S., Sverdrup, H., Kurz, D., & Braun, S. (2011). Exploring Ground Vegetation Change for Different Deposition Scenarios and Methods for Estimating Critical Loads for Biodiversity Using the ForSAFE-VEG Model in Switzerland and Sweden. *Water, Air, & Soil Pollution*, 216(1), 289–317. <https://doi.org/10.1007/s11270-010-0534-6>

Belyazid, S., & Zanchi, G. (2019). Water limitation can negate the effect of higher temperatures on forest carbon sequestration. *European Journal of Forest Research*, 138(2), 287–297. <https://doi.org/10.1007/s10342-019-01168-4>

Blaško, R., Forsmark, B., Gundale, M. J., Lim, H., Lundmark, T., & Nordin, A. (2022). The carbon sequestration response of aboveground biomass and soils to nutrient enrichment in boreal forests depends on baseline site productivity. *Science of The Total Environment*, 838, 156327. <https://doi.org/10.1016/j.scitotenv.2022.156327>

Butlers, A., Laiho, R., Soosaar, K., Jauhiainen, J., Schindler, T., Bārdule, A., Kamil-Sardar, M., Haberl, A., Samariks, V., Vahter, H., Lazdiņš, A., Čiuldienė, D., Armolaitis, K., & Līcīte, I. (2024). Soil and forest floor carbon balance in drained and undrained hemiboreal peatland forests. *EGU sphere*, 1–21. <https://doi.org/10.5194/egusphere-2024-1397>

Chaudhary, N., Zhang, W., Lamba, S., & Westermann, S. (2022). Modeling Pan-Arctic Peatland Carbon Dynamics Under Alternative Warming Scenarios. *Geophysical Research Letters*, 49(10), e2021GL095276. <https://doi.org/10.1029/2021GL095276>

Crusius, J. (2020). “Natural” Climate Solutions Could Speed Up Mitigation, With Risks. Additional Options Are Needed. *Earths Future*, 8(4), UNSP e2019EF001310. <https://doi.org/10.1029/2019EF001310>

Cui, S., Liu, P., Guo, H., Nielsen, C. K., Pullens, J. W. M., Chen, Q., Pugliese, L., & Wu, S. (2024). Wetland hydrological dynamics and methane emissions. *Communications Earth & Environment*, 5(1), 1–17. <https://doi.org/10.1038/s43247-024-01635-w>

Darusman, T., Murdiyarto, D., Impron, & Anas, I. (2023). Effect of rewetting degraded peatlands on carbon fluxes: A meta-analysis. *Mitigation and Adaptation Strategies for Global Change*, 28(3), 10. <https://doi.org/10.1007/s11027-023-10046-9>

- de Bruijn, A., Gustafson, E. J., Sturtevant, B. R., Foster, J. R., Miranda, B. R., Lichti, N. I., & Jacobs, D. F. (2014). Toward more robust projections of forest landscape dynamics under novel environmental conditions: Embedding PnET within LANDIS-II. *Ecological Modelling*, 287, 44–57. <https://doi.org/10.1016/j.ecolmodel.2014.05.004>
- Didion, M., Frey, B., Rogiers, N., & Thürig, E. (2014). Validating tree litter decomposition in the Yasso07 carbon model. *Ecological Modelling*, 291, 58–68. <https://doi.org/10.1016/j.ecolmodel.2014.07.028>
- 1005 [Donohue, R. J., Roderick, M. L., McVicar, T. R., & Yang, Y. \(2017\). A simple hypothesis of how leaf and canopy-level transpiration and assimilation respond to elevated CO2 reveals distinct response patterns between disturbed and undisturbed vegetation. \*Journal of Geophysical Research: Biogeosciences\*, 122\(1\), 168–184. <https://doi.org/10.1002/2016JG003505>](https://doi.org/10.1002/2016JG003505)
- 1010 Engardt, M., & Langner, J. (2013). Simulations of future sulphur and nitrogen deposition over Europe using meteorological data from three regional climate projections. *Tellus. Series B, Chemical and Physical Meteorology*, 65. <https://urn.kb.se/resolve?urn=urn:nbn:se:smhi:diva-419>
- Eriksson, S. (2021). *En laboratoriestudie om kol-, kväve- och fosforcykeln: Med fokus på kväveminalisation*. INSTITUTIONEN FÖR BIOLOGI OCH MILJÖVETENSKAP.
- 1015 Ernfors, M., Rütting, T., & Klemetsson, L. (2011). Increased nitrous oxide emissions from a drained organic forest soil after exclusion of ectomycorrhizal mycelia. *Plant and Soil*, 343(1), 161–170. <https://doi.org/10.1007/s11104-010-0667-9>
- Escobar, D., Belyazid, S., & Manzoni, S. (2022). Back to the Future: Restoring Northern Drained Forested Peatlands for Climate Change Mitigation. *Frontiers in Environmental Science*, 10. <https://www.frontiersin.org/article/10.3389/fenvs.2022.834371>
- 1020 Evans, C. D., Peacock, M., Baird, A. J., Artz, R. R. E., Burden, A., Callaghan, N., Chapman, P. J., Cooper, H. M., Coyle, M., Craig, E., Cumming, A., Dixon, S., Gauci, V., Grayson, R. P., Helfter, C., Heppell, C. M., Holden, J., Jones, D. L., Kaduk, J., ... Morrison, R. (2021). Overriding water table control on managed peatland greenhouse gas emissions. *Nature*, 593(7860), Article 7860. <https://doi.org/10.1038/s41586-021-03523-1>
- Evans, C. D., Renou-Wilson, F., & Strack, M. (2016). The role of waterborne carbon in the greenhouse gas balance of drained and re-wetted peatlands. *Aquatic Sciences*, 78(3), 573–590. <https://doi.org/10.1007/s00027-015-0447-y>
- 1025

Fan, Z., Neff, J. C., Waldrop, M. P., Ballantyne, A. P., & Turetsky, M. R. (2014). Transport of oxygen in soil pore-water systems: Implications for modeling emissions of carbon dioxide and methane from peatlands. *Biogeochemistry*, 121(3), 455–470. <https://doi.org/10.1007/s10533-014-0012-0>

1030 [Fearnside, P. M., Lashof, D. A., & Moura-Costa, P. \(2000\). Accounting for time in Mitigating Global Warming through land-use change and forestry. \*Mitigation and Adaptation Strategies for Global Change\*, 5\(3\), 239–270. <https://doi.org/10.1023/A:1009625122628>](#)

Frolking, S., Roulet, N. T., Tuittila, E., Bubier, J. L., Quillet, A., Talbot, J., & Richard, P. J. H. (2010). A new model of Holocene peatland net primary production, decomposition, water balance, and peat accumulation. *Earth System Dynamics*, 1(1), 1–21. <https://doi.org/10.5194/esd-1-1-2010>

1035 Guenther, A., Barthelmes, A., Huth, V., Joosten, H., Jurasinski, G., Koebisch, F., & Couwenberg, J. (2020). Prompt rewetting of drained peatlands reduces climate warming despite methane emissions. *Nature Communications*, 11(1), 1644. <https://doi.org/10.1038/s41467-020-15499-z>

Gundale, M. J., Axelsson, E. P., Buness, V., Callebaut, T., DeLuca, T. H., Hupperts, S. F., Ibáñez, T. S., Metcalfe, D. B., Nilsson, M.-C., Peichl, M., Spitzer, C. M., Stangl, Z. R., Strengbom, J., Sundqvist, M. K., Wardle, D. A., & Lindahl, 1040 B. D. (2024). The biological controls of soil carbon accumulation following wildfire and harvest in boreal forests: A review. *Global Change Biology*, 30(5), e17276. <https://doi.org/10.1111/gcb.17276>

Gustafson, E. J., [Kubiske, M. E., Miranda, B. R., Hoshika, Y., & Paoletti, E. \(2018\). Extrapolating plot-scale CO2 and ozone enrichment experimental results to novel conditions and scales using mechanistic modeling. \*Ecological Processes\*, 7\(1\), 31. <https://doi.org/10.1186/s13717-018-0142-8>](#)

1045 [Gustafson, E. J., Miranda, B. R., Shvidenko, A. Z., & Sturtevant, B. R. \(2020\). Simulating Growth and Competition on Wet and Waterlogged Soils in a Forest Landscape Model. \*Frontiers in Ecology and Evolution\*, 8. <https://doi.org/10.3389/fevo.2020.598775>](#)

Haapalehto, T., Kotiaho, J. S., Matilainen, R., & Tahvanainen, T. (2014). The effects of long-term drainage and subsequent restoration on water table level and pore water chemistry in boreal peatlands. *Journal of Hydrology*, 519, 1493–1505. 1050 <https://doi.org/10.1016/j.jhydrol.2014.09.013>

- Hansson, K., Fröberg, M., Helmisaari, H.-S., Kleja, D. B., Olsson, B. A., Olsson, M., & Persson, T. (2013). Carbon and nitrogen pools and fluxes above and below ground in spruce, pine and birch stands in southern Sweden. *Forest Ecology and Management*, 309, 28–35. <https://doi.org/10.1016/j.foreco.2013.05.029>
- He, H., Jansson, P.-E., Svensson, M., Björklund, J., Tarvainen, L., Klemedtsson, L., & Kasimir, Å. (2016). Forests on drained agricultural peatland are potentially large sources of greenhouse gases – insights from a full rotation period simulation. *Biogeosciences*, 13(8), 2305–2318. <https://doi.org/10.5194/bg-13-2305-2016>
- Hermans, R., McKenzie, R., Andersen, R., Teh, Y. A., Cowie, N., & Subke, J.-A. (2022). Net soil carbon balance in afforested peatlands and separating autotrophic and heterotrophic soil CO<sub>2</sub> effluxes. *Biogeosciences*, 19(2), 313–327. <https://doi.org/10.5194/bg-19-313-2022>
- Hilli, S. (2013). *Significance of litter production of forest stands and ground vegetation in the formation of organic matter and storage of carbon in boreal coniferous forests*. <https://jukuri.luke.fi/handle/10024/554803>
- Hökkä, H., Stenberg, L., & Laurén, A. (2020). Modeling depth of drainage ditches in forested peatlands in Finland. *Baltic Forestry*, 26(2), Article 2. <https://doi.org/10.46490/BF453>
- Jauhiainen, J., Heikkinen, J., Clarke, N., He, H., Dalsgaard, L., Minkinen, K., Ojanen, P., Vesterdal, L., Alm, J., Butlers, A., Callesen, I., Jordan, S., Lohila, A., Mander, Ü., Óskarsson, H., Sigurdsson, B. D., Sjøgaard, G., Soosaar, K., Kasimir, Å., ... Laiho, R. (2023). Reviews and syntheses: Greenhouse gas emissions from drained organic forest soils – synthesizing data for site-specific emission factors for boreal and cool temperate regions. *Biogeosciences*, 20(23), 4819–4839. <https://doi.org/10.5194/bg-20-4819-2023>
- Jílková, V., Jandová, K., Cajthaml, T., Kukla, J., & Jansa, J. (2022). Differences in the flow of spruce-derived needle leachates and root exudates through a temperate coniferous forest mineral topsoil. *Geoderma*, 405, 115441. <https://doi.org/10.1016/j.geoderma.2021.115441>
- Jonsson, R., Blujdea, V. N. B., Fiorese, G., Pilli, R., Rinaldi, F., Baranzelli, C., & Camia, A. (2018). Outlook of the European forest-based sector: Forest growth, harvest demand, wood-product markets, and forest carbon dynamics implications. *iForest - Biogeosciences and Forestry*, 11(2), 315. <https://doi.org/10.3832/ifor2636-011>

- 1075 Joos, F., Roth, R., Fuglestad, J. S., Peters, G. P., Enting, I. G., von Bloh, W., Brovkin, V., Burke, E. J., Eby, M., Edwards, N. R., Friedrich, T., Frölicher, T. L., Halloran, P. R., Holden, P. B., Jones, C., Kleinen, T., Mackenzie, F. T., Matsumoto, K., Meinshausen, M., ... Weaver, A. J. (2013). Carbon dioxide and climate impulse response functions for the computation of greenhouse gas metrics: A multi-model analysis. *Atmospheric Chemistry and Physics*, 13(5), 2793–2825. <https://doi.org/10.5194/acp-13-2793-2013>
- 1080 Jovani-Sancho, A. J., Cummins, T., & Byrne, K. A. (2021). Soil carbon balance of afforested peatlands in the maritime temperate climatic zone. *Global Change Biology*, 27(15), 3681–3698. <https://doi.org/10.1111/gcb.15654>
- Kasimir, Å., He, H., Coria, J., & Nordén, A. (2018). Land use of drained peatlands: Greenhouse gas fluxes, plant production, and economics. *Global Change Biology*, 24(8), 3302–3316. <https://doi.org/10.1111/gcb.13931>
- 1085 [Kilpeläinen, J., Peltoniemi, K., Ojanen, P., Mäkiranta, P., Adamczyk, S., Domisch, T., Laiho, R., & Adamczyk, B. \(2023\). Waterlogging may reduce chemical soil C stabilization in forested peatlands. \*Soil Biology and Biochemistry\*, 187, 109229. <https://doi.org/10.1016/j.soilbio.2023.109229>](#)
- Kleinen, T., Brovkin, V., & Schuldt, R. J. (2012). A dynamic model of wetland extent and peat accumulation: Results for the Holocene. *Biogeosciences*, 9(1), 235–248. <https://doi.org/10.5194/bg-9-235-2012>
- 1090 [Kleja, D. B., Svensson, M., Majdi, H., Jansson, P.-E., Langvall, O., Bergkvist, B., Johansson, M.-B., Weslien, P., Truusb, L., Lindroth, A., & Ågren, G. I. \(2008\). Pools and fluxes of carbon in three Norway spruce ecosystems along a climatic gradient in Sweden. \*Biogeochemistry\*, 89\(1\), 7–25. <https://doi.org/10.1007/s10533-007-9136-9>](#)
- Klemetsson, L., Ernfors, M., Björk, R. G., Weslien, P., Rütting, T., Crill, P., & Sikström, U. (2010). Reduction of greenhouse gas emissions by wood ash application to a *Picea abies* (L.) Karst. Forest on a drained organic soil. *European Journal of Soil Science*, 61(5), 734–744. <https://doi.org/10.1111/j.1365-2389.2010.01279.x>
- 1095 [Klemetsson, L., Weslien, P., Bastviken, D., Natchimuthu, S., & Wallin, M. \(2015\). \*The Skogaryd Research Catchment—An infrastructure to integrate terrestrial and aquatic greenhouse gas fluxes\*. 7461. EGU General Assembly Conference Abstracts. <https://ui.adsabs.harvard.edu/abs/2015EGUGA..17.7461K>](#)
- Korkiakoski, M., Ojanen, P., Tuovinen, J.-P., Minkinen, K., Nevalainen, O., Penttilä, T., Aurela, M., Laurila, T., & Lohila, A. (2023). Partial cutting of a boreal nutrient-rich peatland forest causes radically less short-term on-site CO<sub>2</sub>



emissions than clear-cutting. *Agricultural and Forest Meteorology*, 332, 109361. <https://doi.org/10.1016/j.agrformet.2023.109361>

Korkiakoski, M., Tuovinen, J.-P., Penttilä, T., Sarkkola, S., Ojanen, P., Minkkinen, K., Rainne, J., Laurila, T., & Lohila, A. (2019). Greenhouse gas and energy fluxes in a boreal peatland forest after clear-cutting. *Biogeosciences*, 16(19), 3703–3723. <https://doi.org/10.5194/bg-16-3703-2019>

Krause, A., Knoke, T., & Rammig, A. (2020). A regional assessment of land-based carbon mitigation potentials: Bioenergy, BECCS, reforestation, and forest management. *Global Change Biology Bioenergy*, 12(5), 346–360. <https://doi.org/10.1111/gcbb.12675>

Kreyling, J., Tanneberger, F., Jansen, F., van der Linden, S., Aggenbach, C., Blüml, V., Couwenberg, J., Emsens, W.-J., Joosten, H., Klimkowska, A., Kotowski, W., Kozub, L., Lennartz, B., Liczner, Y., Liu, H., Michaelis, D., Oehmke, C., Parakenings, K., Pleyl, E., ... Jurasinski, G. (2021). Rewetting does not return drained fen peatlands to their old selves. *Nature Communications*, 12(1), 5693. <https://doi.org/10.1038/s41467-021-25619-y>

Laine, J., Laiho, R., Minkkinen, K., & Vasander, H. (2006). Forestry and Boreal Peatlands. In R. K. Wieder & D. H. Vitt (Eds.), *Boreal Peatland Ecosystems* (pp. 331–357). Springer. [https://doi.org/10.1007/978-3-540-31913-9\\_15](https://doi.org/10.1007/978-3-540-31913-9_15)

Laudon, H., & Maher Hasselquist, E. (2023). Applying continuous-cover forestry on drained boreal peatlands; water regulation, biodiversity, climate benefits and remaining uncertainties. *Trees, Forests and People*, 11, 100363. <https://doi.org/10.1016/j.tfp.2022.100363>

Lazdiņš, A., Lupiķis, A., Polmanis, K., Bārdule, A., Butlers, A., & Kalēja, S. (2024). Carbon stock changes of drained nutrient-rich organic forest soils in Latvia. *Silva Fennica*, 58(1). <https://www.silvafennica.fi/article/22017>

Lehtonen, A., Eyvindson, K., Härkönen, K., Leppä, K., Salmivaara, A., Peltoniemi, M., Salminen, O., Sarkkola, S., Launiainen, S., Ojanen, P., Rätty, M., & Mäkipää, R. (2023). Potential of continuous cover forestry on drained peatlands to increase the carbon sink in Finland. *Scientific Reports*, 13(1), 15510. <https://doi.org/10.1038/s41598-023-42315-7>

Leifeld, J., Wüst-Galley, C., & Page, S. (2019). Intact and managed peatland soils as a source and sink of GHGs from 1850 to 2100. *Nature Climate Change*, 9(12), 945–947. <https://doi.org/10.1038/s41558-019-0615-5>

- 1125 Leppä, K., Hökkä, H., Laiho, R., Launiainen, S., Lehtonen, A., Mäkipää, R., Peltoniemi, M., Saarinen, M., Sarkkola, S., &  
Nieminen, M. (2020). Selection Cuttings as a Tool to Control Water Table Level in Boreal Drained Peatland Forests.  
*Frontiers in Earth Science*, 8. <https://doi.org/10.3389/feart.2020.576510>
- Leppälampi-Kujansuu, J., Salemaa, M., Kleja, D. B., Linder, S., & Helmisaari, H.-S. (2014). Fine root turnover and litter  
production of Norway spruce in a long-term temperature and nutrient manipulation experiment. *Plant and Soil*,  
1130 374(1), 73–88. <https://doi.org/10.1007/s11104-013-1853-3>
- Li, J., Zhou, M., Alaei, S., & Bengtson, P. (2020). Rhizosphere priming effects differ between Norway spruce (*Picea abies*)  
and Scots pine seedlings cultivated under two levels of light intensity. *Soil Biology and Biochemistry*, 145, 107788.  
<https://doi.org/10.1016/j.soilbio.2020.107788>
- Liu, H., Price, J., Rezanezhad, F., & Lennartz, B. (2020). Centennial-Scale Shifts in Hydrophysical Properties of Peat Induced  
by Drainage. *Water Resources Research*, 56(10), e2020WR027538. <https://doi.org/10.1029/2020WR027538>
- 1135 Maljanen, M., Shurpali, N., Hytönen, J., Mäkiranta, P., Aro, L., Potila, H., Laine, J., Li, C., & Martikainen, P. J. (2012).  
Afforestation does not necessarily reduce nitrous oxide emissions from managed boreal peat soils. *Biogeochemistry*,  
108(1/3), 199–218. <https://www.jstor.org/stable/41410591>
- Mamkin, V., Avilov, V., Ivanov, D., Varlagin, A., & Kurbatova, J. (2023). Interannual variability in the ecosystem CO<sub>2</sub> fluxes  
at a paludified spruce forest and ombrotrophic bog in the southern taiga. *Atmospheric Chemistry and Physics*, 23(3),  
2273–2291. <https://doi.org/10.5194/acp-23-2273-2023>
- Manzoni, S., Čapek, P., Porada, P., Thurner, M., Winterdahl, M., Beer, C., Brüchert, V., Frouz, J., Herrmann, A. M., Lindahl,  
B. D., Lyon, S. W., Šantrůčková, H., Vico, G., & Way, D. (2018). Reviews and syntheses: Carbon use efficiency  
from organisms to ecosystems – definitions, theories, and empirical evidence. *Biogeosciences*, 15(19), 5929–5949.  
1145 <https://doi.org/10.5194/bg-15-5929-2018>
- Menberu, M. W., Tahvanainen, T., Marttila, H., Irannezhad, M., Ronkanen, A.-K., Penttinen, J., & Kløve, B. (2016). Water-  
table-dependent hydrological changes following peatland forestry drainage and restoration: Analysis of restoration  
success. *Water Resources Research*, 52(5), 3742–3760. <https://doi.org/10.1002/2015WR018578>

- Metzler, H., Launiainen, S., & Vico, G. (2024). Amount of carbon fixed, transit time and fate of harvested wood products define the climate change mitigation potential of boreal forest management—A model analysis. *Ecological Modelling*, 491, 110694. <https://doi.org/10.1016/j.ecolmodel.2024.110694>
- Meyer, A., Tarvainen, L., Noursratpour, A., Björk, R. G., Ernfors, M., Grelle, A., Kasimir Klemetsson, Å., Lindroth, A., Räntfors, M., Rütting, T., Wallin, G., Weslien, P., & Klemetsson, L. (2013). A fertile peatland forest does not constitute a major greenhouse gas sink. *Biogeosciences*, 10(11), 7739–7758. <https://doi.org/10.5194/bg-10-7739-2013>
- Minkkinen, K., Laine, J., Shurpali, N. J., Mäkiranta, P., Alm, J., & Penttilä, T. (2007). *Heterotrophic soil respiration in forestry-drained peatlands*. <https://jukuri.luke.fi/handle/10024/513693>
- Minkkinen, K., Ojanen, P., Koskinen, M., & Penttilä, T. (2020). Nitrous oxide emissions of undrained, forestry-drained, and rewetted boreal peatlands. *Forest Ecology and Management*, 478, 118494. <https://doi.org/10.1016/j.foreco.2020.118494>
- Minkkinen, K., Ojanen, P., Penttilä, T., Aurela, M., Laurila, T., Tuovinen, J.-P., & Lohila, A. (2018). Persistent carbon sink at a boreal drained bog forest. *BIOGEOSCIENCES*, 15(11), 3603–3624. <https://doi.org/10.5194/bg-15-3603-2018>
- Muñoz, E., Chanca, I., González-Sosa, M., Sarquis, A., Tangarife-Escobar, A., & Sierra, C. A. (2024). On the importance of time in carbon sequestration in soils and climate change mitigation. *Global Change Biology*, 30(3), e17229. <https://doi.org/10.1111/gcb.17229>
- Munthe, J., Arnell, J., Moldan, F., Karlsson, P. E., Åström, S., Gustafsson, T., Kindbom, K., Hellsten, S., Hansen, K., Jutterström, S., Lindblad, M., Tekie, H., Malmaeus, M., & Kronnäs, V. (2016). *Klimatförändringen och miljömål*. IVL Svenska Miljöinstitutet. <https://urn.kb.se/resolve?urn=urn:nbn:se:ivl:diva-356>
- Murphy, D. M., & Ravishankara, A. R. (2018). Trends and patterns in the contributions to cumulative radiative forcing from different regions of the world. *Proceedings of the National Academy of Sciences*, 115(52), 13192–13197. <https://doi.org/10.1073/pnas.1813951115>

- Nieminen, M., Piirainen, S., Sikström, U., Löfgren, S., Marttila, H., Sarkkola, S., Laurén, A., & Finér, L. (2018). Ditch network maintenance in peat-dominated boreal forests: Review and analysis of water quality management options. *Ambio*, 47(5), 535–545. <https://doi.org/10.1007/s13280-018-1047-6>
- 1175 Noebel, R. (2023). *WHY IS PEATLAND REWETTING CRITICAL FOR MEETING EU ENVIRONMENTAL OBJECTIVES?* IEEP.
- Nyström, E. (2016). *The Geology of the Skogaryd Research Catchment, Sweden: A Basis for Future Hydrogeological Research*. Department of Earth Sciences, University of Gothenburg.
- ~~Ogle, K., & Pacala, S. W. (2009). A modeling framework for inferring tree growth and allocation from physiological, morphological and allometric traits. *Tree Physiology*, 29(4), 587–605. <https://doi.org/10.1093/treephys/tpn051>~~
- 1180 ~~morphological and allometric traits. *Tree Physiology*, 29(4), 587–605. <https://doi.org/10.1093/treephys/tpn051>~~
- Ojanen, P., & Minkkinen, K. (2019). The dependence of net soil CO<sub>2</sub> emissions on water table depth in boreal peatlands drained for forestry. *MIRES AND PEAT*, 24, 27. <https://doi.org/10.19189/MaP.2019.OMB.StA.1751>
- Ojanen, P., & Minkkinen, K. (2020). Rewetting Offers Rapid Climate Benefits for Tropical and Agricultural Peatlands But Not for Forestry-Drained Peatlands. *Global Biogeochemical Cycles*, 34(7), e2019GB006503. <https://doi.org/10.1029/2019GB006503>
- 1185 <https://doi.org/10.1029/2019GB006503>
- Ojanen, P., Minkkinen, K., Alm, J., & Penttilä, T. (2010). Soil–atmosphere CO<sub>2</sub>, CH<sub>4</sub> and N<sub>2</sub>O fluxes in boreal forestry-drained peatlands. *Forest Ecology and Management*, 260(3), 411–421. <https://doi.org/10.1016/j.foreco.2010.04.036>
- Palviainen, M., Peltomaa, E., Laurén, A., Kinnunen, N., Ojala, A., Berninger, F., Zhu, X., & Pumpanen, J. (2022). Water quality and the biodegradability of dissolved organic carbon in drained boreal peatland under different forest harvesting intensities. *Science of The Total Environment*, 806, 150919. <https://doi.org/10.1016/j.scitotenv.2021.150919>
- 1190 <https://doi.org/10.1016/j.scitotenv.2021.150919>
- Prescott, C. E., Grayston, S. J., Helmisaari, H.-S., Kaštovská, E., Körner, C., Lambers, H., Meier, I. C., Millard, P., & Ostonen, I. (2020). Surplus Carbon Drives Allocation and Plant–Soil Interactions. *Trends in Ecology & Evolution*, 35(12), 1110–1118. <https://doi.org/10.1016/j.tree.2020.08.007>
- 1195 Profft, I., Mund, M., Weber, G.-E., Weller, E., & Schulze, E.-D. (2009). Forest management and carbon sequestration in wood products. *European Journal of Forest Research*, 128(4), 399–413. <https://doi.org/10.1007/s10342-009-0283-5>

- Qiu, C., Zhu, D., Ciais, P., Guenet, B., Krinner, G., Peng, S., Aurela, M., Bernhofer, C., Brümmer, C., Bret-Harte, S., Chu, H., Chen, J., Desai, A. R., Dušek, J., Euskirchen, E. S., Fortuniak, K., Flanagan, L. B., Friborg, T., Grygoruk, M., ... Ziemblinska, K. (2018). ORCHIDEE-PEAT (revision 4596), a model for northern peatland CO<sub>2</sub>, water, and energy fluxes on daily to annual scales. *Geoscientific Model Development*, 11(2), 497–519. <https://doi.org/10.5194/gmd-11-497-2018>
- Ranniku, R., Mander, Ü., Escuer-Gatius, J., Schindler, T., Kupper, P., Sellin, A., & Soosaar, K. (2024). Dry and wet periods determine stem and soil greenhouse gas fluxes in a northern drained peatland forest. *Science of The Total Environment*, 928, 172452. <https://doi.org/10.1016/j.scitotenv.2024.172452>
- Reddy, K. R., & DeLaune, R. D. (2008). Carbon. In *Biogeochemistry of Wetlands*. CRC Press.
- Rewcastle, K. E., Moore, J. A. M., Henning, J. A., Mayes, M. A., Patterson, C. M., Wang, G., Metcalfe, D. B., & Classen, A. T. (2020). Investigating drivers of microbial activity and respiration in a forested bog. *Pedosphere*, 30(1), 135–145. [https://doi.org/10.1016/S1002-0160\(19\)60841-6](https://doi.org/10.1016/S1002-0160(19)60841-6)
- Rogelj, J., Shindell, D., Jiang, K., Fifita, S., Forster, P., Ginzburg, V., Handa, C., Kobayashi, S., Kriegler, E., Mundaca, L., Séférian, R., Vilarinho, M. V., Calvin, K., Emmerling, J., Fuss, S., Gillett, N., He, C., Hertwich, E., Höglund-Isaksson, L., ... Schaeffer, R. (2018). *Mitigation Pathways Compatible with 1.5°C in the Context of Sustainable Development* (p. 82). IPCC.
- Sabbatini, S., Mammarella, I., Arriga, N., Fratini, G., Graf, A., Hörtnagl, L., Ibrom, A., Longdoz, B., Mauder, M., Merbold, L., Metzger, S., Montagnani, L., Pitacco, A., Rebmann, C., Sedlak, P., Sigut, L., Vitale, D., & Papale, D. (2018). Eddy covariance raw data processing for CO<sub>2</sub> and energy fluxes calculation at ICOS ecosystem stations. *International Agrophysics*, 32(4), 495–515. <https://doi.org/10.1515/intag-2017-0043>
- Seddon, N., Chausson, A., Berry, P., Girardin, C. A. J., Smith, A., & Turner, B. (2020). Understanding the value and limits of nature-based solutions to climate change and other global challenges. *Philosophical Transactions of the Royal Society B-Biological Sciences*, 375(1794), 20190120. <https://doi.org/10.1098/rstb.2019.0120>
- Sierra, C. A. (2024). Integrating time in definitions of carbon sequestration and greenhouse gas removals and reversals. *In Review in Royal Society Open Science*.

Sierra, C. A., Crow, S. E., Heimann, M., Metzler, H., & Schulze, E.-D. (2021). The climate benefit of carbon sequestration. *Biogeosciences*, 18(3), 1029–1048. <https://doi.org/10.5194/bg-18-1029-2021>

Sigurdsson, B. D., Medhurst, J. L., Wallin, G., Eggertsson, O., & Linder, S. (2013). Growth of mature boreal Norway spruce was not affected by elevated [CO<sub>2</sub>] and/or air temperature unless nutrient availability was improved. *Tree Physiology*, 33(11), 1192–1205. <https://doi.org/10.1093/treephys/tpt043>

Sigurdsson, B. D., Roberitz, P., Freeman, M., Næss, M., Saxe, H., Thorgeirsson, H., & Linder, S. (2002). Impact studies on Nordic forests: Effects of elevated CO<sub>2</sub> and fertilization on gas exchange. *Canadian Journal of Forest Research*, 32(5), 779–788. Scopus. <https://doi.org/10.1139/x01-114>

Silins, U., & Rothwell, R. L. (1998). Forest Peatland Drainage and Subsidence Affect Soil Water Retention and Transport Properties in an Alberta Peatland. *Soil Science Society of America Journal*, 62(4), 1048–1056. <https://doi.org/10.2136/sssaj1998.03615995006200040028x>

Tanneberger, F., Appulo, L., Ewert, S., Lakner, S., Ó Brolcháin, N., Peters, J., & Wichtmann, W. (2021). The Power of Nature-Based Solutions: How Peatlands Can Help Us to Achieve Key EU Sustainability Objectives. *Advanced Sustainable Systems*, 5(1), 2000146. <https://doi.org/10.1002/adsu.202000146>

Tong, C. H. M., Noumonvi, K. D., Ratcliffe, J., Laudon, H., Järveoja, J., Drott, A., Nilsson, M. B., & Peichl, M. (2024). A drained nutrient-poor peatland forest in boreal Sweden constitutes a net carbon sink after integrating terrestrial and aquatic fluxes. *Global Change Biology*, 30(3), e17246. <https://doi.org/10.1111/gcb.17246>

Ťupek, B., Lehtonen, A., Yurova, A., Abramoff, R., Manzoni, S., Guenet, B., Bruni, E., Launiainen, S., Peltoniemi, M., Hashimoto, S., Tian, X., Heikkinen, J., Minkinen, K., & Mäkipää, R. (2023). Modeling boreal forest’s mineral soil and peat C stock dynamics with Yasso07 model coupled with updated moisture modifier. *EGUsphere*, 1–34. <https://doi.org/10.5194/egusphere-2023-1523>

Uddling, J., & Wallin, G. (2012). Interacting effects of elevated CO<sub>2</sub> and weather variability on photosynthesis of mature boreal Norway spruce agree with biochemical model predictions. *Tree Physiology*, 32(12), 1509–1521. <https://doi.org/10.1093/treephys/tps086>

Ukonmaanaho, L., Merilä, P., Nöjd, P., & Nieminen, T. M. (2008). *Litterfall production and nutrient return to the forest floor in Scots pine and Norway spruce stands in Finland*. <https://jukuri.luke.fi/handle/10024/514741>

Uri, V., Kukumagi, M., Aosaar, J., Varik, M., Becker, H., Morozov, G., & Karoles, K. (2017). Ecosystems carbon budgets of differently aged downy birch stands growing on well-drained peatlands. *Forest Ecology and Management*, 399, 82–93. <https://doi.org/10.1016/j.foreco.2017.05.023>

Vestin, P., Mölder, M., Kljun, N., Cai, Z., Hasan, A., Holst, J., Klemetsson, L., & Lindroth, A. (2020). Impacts of Clear-Cutting of a Boreal Forest on Carbon Dioxide, Methane and Nitrous Oxide Fluxes. *Forests*, 11(9), Article 9. <https://doi.org/10.3390/f11090961>

Wallman, P., Svensson, M. G. E., Sverdrup, H., & Belyazid, S. (2005). ForSAFE—an integrated process-oriented forest model for long-term sustainability assessments. *Forest Ecology and Management*, 207(1), 19–36. <https://doi.org/10.1016/j.foreco.2004.10.016>

Wilson, D., Blain, D., Couwenberg, J., Evans, C. D., Murdiyarso, D., Page, S. E., Renou-Wilson, F., Rieley, J. O., Sirin, A., Strack, M., & Tuittila, E.-S. (2016). Greenhouse gas emission factors associated with rewetting of organic soils. *Mires and Peat*, 17. <https://doi.org/10.19189/MaP.2016.OMB.222>

Wutzler, T., Lucas-Moffat, A., Migliavacca, M., Knauer, J., Sickel, K., Šigut, L., Menzer, O., & Reichstein, M. (2018). Basic and extensible post-processing of eddy covariance flux data with REddyProc. *Biogeosciences*, 15(16), 5015–5030. <https://doi.org/10.5194/bg-15-5015-2018>

Yu, L., Zanchi, G., Akselsson, C., Wallander, H., & Belyazid, S. (2018). Modeling the forest phosphorus nutrition in a southwestern Swedish forest site. *Ecological Modelling*, 369, 88–100. <https://doi.org/10.1016/j.ecolmodel.2017.12.018>

Zanchi, G., Lucander, K., Kronnäs, V., Lampa, M. E., & Akselsson, C. (2021). Modelling the effects of forest management intensification on base cation concentrations in soil water and on tree growth in spruce forests in Sweden. *European Journal of Forest Research*, 140(6), 1417–1429. <https://doi.org/10.1007/s10342-021-01408-6>

Zanchi, G., Yu, L., Akseelsson, C., Bishop, K., Köhler, S., Olofsson, J., & Belyazid, S. (2021). Simulation of water and chemical transport of chloride from the forest ecosystem to the stream. *Environmental Modelling & Software*, 138, 104984. <https://doi.org/10.1016/j.envsoft.2021.104984>

1270  
1275  
1280  
1285  
1290